Journal of Medicinal Chemistry

Subscriber access provided by McMaster University Library

Article

Design, Synthesis, and Biological Evaluation of 1-Phenylpyrazolo[3,4-*e*]pyrrolo[3,4-*g*]indolizine-4,6(1*H*,5*H*)-diones as New Glycogen Synthase Kinase-3# Inhibitors

Valeria La Pietra, Giuseppe La Regina, Antonio Coluccia, Valeria Famiglini, Sveva Pelliccia, Batya Plotkin, Hagit Eldar-Finkelman, Andrea Brancale, Carlo Ballatore, Alex Crowe, Kurt R Brunden, Luciana Marinelli, Ettore Novellino, and Romano Silvestri

J. Med. Chem., **Just Accepted Manuscript** • Publication Date (Web): 02 Dec 2013

Downloaded from http://pubs.acs.org on December 10, 2013

Just Accepted

"Just Accepted" manuscripts have been peer-reviewed and accepted for publication. They are posted online prior to technical editing, formatting for publication and author proofing. The American Chemical Society provides "Just Accepted" as a free service to the research community to expedite the dissemination of scientific material as soon as possible after acceptance. "Just Accepted" manuscripts appear in full in PDF format accompanied by an HTML abstract. "Just Accepted" manuscripts have been fully peer reviewed, but should not be considered the official version of record. They are accessible to all readers and citable by the Digital Object Identifier (DOI®). "Just Accepted" is an optional service offered to authors. Therefore, the "Just Accepted" Web site may not include all articles that will be published in the journal. After a manuscript is technically edited and formatted, it will be removed from the "Just Accepted" Web site and published as an ASAP article. Note that technical editing may introduce minor changes to the manuscript text and/or graphics which could affect content, and all legal disclaimers and ethical guidelines that apply to the journal pertain. ACS cannot be held responsible for errors or consequences arising from the use of information contained in these "Just Accepted" manuscripts.

ACS Publications
High quality. High impact.

Journal of Medicinal Chemistry is published by the American Chemical Society. 1155 Sixteenth Street N.W., Washington, DC 20036

Published by American Chemical Society. Copyright © American Chemical Society. However, no copyright claim is made to original U.S. Government works, or works produced by employees of any Commonwealth realm Crown government in the course of their duties.

Design, Synthesis, and Biological Evaluation of 1-Phenylpyrazolo[3,4-*e*]pyrrolo[3,4-*g*]indolizine-4,6(1*H*,5*H*)-diones as New Glycogen Synthase Kinase-3β Inhibitors

Valeria La Pietra,[fi] Giuseppe La Regina,[†,*] Antonio Coluccia,[†] Valeria Famiglini,[†] Sveva Pelliccia,[†] Batya Plotkin,[§] Hagit Eldar-Finkelman,[§] Andrea Brancale,[¶] Carlo Ballatore[†,‡], Alex Crowe[‡], Kurt R. Brunden[‡], Luciana Marinelli,[fi,*] Ettore Novellino,[fi] and Romano Silvestri[†]

[†] Istituto Pasteur – Fondazione Cenci Bolognetti, Dipartimento di Chimica e Tecnologie del Farmaco, Sapienza Università di Roma, Piazzale Aldo Moro 5, I-00185 Roma, Italy

[fi]Dipartimento di Farmacia, Università di Napoli Federico II, Via Domenico Montesano 49, I-80131 Napoli, Italy

[§]Department of Human Molecular Genetics and Biochemistry, Sackler School of Medicine, Tel Aviv University, IL-69978 Tel Aviv, Israel

[¶]Welsh School of Pharmacy, Cardiff University, King Edward VII Avenue, Cardiff, CF10 3NB, UK

[†]Department of Chemistry, School of Arts and Sciences, University of Pennsylvania, 231 South 34th Street, Philadelphia, Pennsylvania 19104, United States

[‡]Center for Neurodegenerative Disease Research, Department of Pathology and Laboratory Medicine, Perelman School of Medicine, University of Pennsylvania, 3600 Spruce Street, Philadelphia, Pennsylvania 19104, United States

ABSTRACT

Compound **5** was selected from our in-house library as a suitable starting point for the rational design of new GSK-3β inhibitors. MC/FEP calculations of **5** led to identify a structural class of new GSK-3β inhibitors. Compound **18** inhibited GSK-3β with IC_{50} of 0.24 μM, and inhibited tau phosphorylation in a cell-based assay. It proved to be a selective inhibitor of GSK-3 against a panel of 17 kinases, and showed >10-fold selectivity against CDK2. Calculated physico-chemical properties and Volsurf predictions suggested that compound **18** has the potential to passively diffuse across the blood-brain barrier.

INTRODUCTION

Alzheimer's disease (AD) is a leading cause of death worldwide. Currently, more than five million people are estimated to suffer from AD and this number will grow significantly over the coming decades. By 2050, there is expected to be nearly a million new cases per year.[1] AD is a devastating dementia condition characterized by a progressive age-related loss of memory and impairment of cognitive capability. The development of AD is accompanied by neuronal loss, which appears to correlate with the appearance of intracellular aggregates of the microtubule-associated protein (MAP) tau (e.g., neurofibrillary tangles, or NFTs).[2] In addition, the AD brain is characterized by the presence of extracellular senile plaques comprised of Aβ peptides.[3,4] Current treatments of AD are not disease-modifying and are merely palliative. There is an unmet need for newer drugs in the treatment of AD as the current options show significant limitations.[5]

Glycogen synthase kinase-3 (GSK-3) is a proline-directed serine/threonine kinase that is expressed as α and β isoforms and which is responsible for the phosphorylation of a variety of cellular substrates and is involved in the molecular pathogenesis of severe human diseases.[6] In the brain, a principal consequence of dysregulation of GSK-3 is the hyperphosphorylation of tau proteins.[7] GSK-3 plays a key role in glucose metabolism as its inhibitory phosphorylation reduces the rate of conversion of glucose to glycogen, thus elevating the glucose concentration in the blood.[8] It is also recognized that that GSK-3 is involved in cell-fate control,[9] insulin signaling cascade,[10] differentiation and proliferation,[11] apoptosis regulation (its inhibition may have a neuroprotective effect),[12] and it may serve as a drug target for amyotrophic lateral sclerosis.[13]

Chart 1. Reference Compounds 1-5, and new Derivatives 6-18.[a]

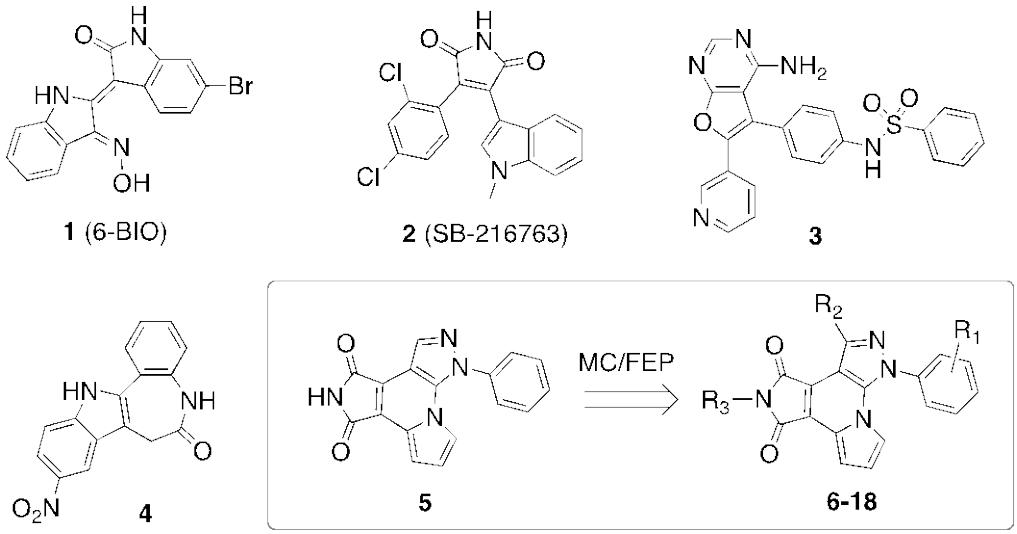

[a] **6**, R_1 = 2-Cl, R_2 = R_3 = H; **7**, R_1 = 3-Cl, R_2 = R_3 = H; **8**, R_1 = 4-Cl, R_2 = R_3 = H; **9**, R_1 = 2-Me, R_2 = R_3 = H; **10**, R_1 = 3-Me, R_2 = R_3 = H; **11**, R_1 = 4-Me, R_2 = R_3 = H; **12**, R_1 = 2-MeO, R_2 = R_3 = H; **13**, R_1 = H, R_2 = Me, R_3 = H; **14**, R_1 = R_2 = H, R_3 = Me; **15**, R_1 = 2-Me, R_2 = Me, R_3 = H; **16**, R_1 = 2-Cl, R_2 = Me, R_3 = H; **17**, R_1 = 4-Cl,2-Me, R_2 = Me, R_3 = H; **18**, R_1 = 2,4-Cl_2, R_2 = Me, R_3 = H;

GSK-3α, GSK-3β share 84% overall identity and >98% identity within their catalytic domains.[14] Both isoforms are highly expressed in the brain and testicles and share similar functions in several cellular processes.[15] GSK-3β represents the predominant isoform present in most CNS areas, where it is localized primarily in neurons.

GSK-3β-mediated hyperphosphorylation of tau has been implicated in the pathogenesis of AD, as hyperphosphorylation promotes the detachment of tau from the microtubules and renders the protein more prone to misfolding and aggregation, thus leading to the formation of NFTs and, ultimately, neuronal death.[16] There is evidence of a correlation between an increase in GSK-3β activity and NFT formation, altered integrity of the microtubule network, and neurodegeneration.[17] As GSK-3β showed

connections to mechanisms involved in AD and other CNS disorders, it has become an attractive target for medicinal chemists both in academia and pharmaceutical companies.[18]

Over the past decades, a number of diverse GSK-3β inhibitors have been reported.[19] We observed that compound **5**, previously synthesized by us,[20] shared some chemical features common with known GSK-3β inhibitors (**1**,[21] **2**,[22] **3**,[23] **4**,[24]) (Chart 1). In a preliminary screening for GSK-3β inhibitory activity, compound **5** showed an IC_{50} of 1.69 μM. These results prompted us to analyse the potential for productive modifications of **5** in a quest to discover new potent GSK-3β inhibitors. Thus, optimization of **5** was initiated using a computationally driven approach, primarily guided by results of free energy perturbation (FEP) calculations for complexes of analogues of **5** with GSK-3β.[25]

CHEMISTRY

The synthesis of 1-(phenyl)pyrazolo[3,4-*e*]pyrrolo[3,4-*g*]indolizine-4,6(1*H*,5*H*)-dione derivatives **5**-**18** is depicted in Scheme 1. Sodium dicyanoalk-1-en-1-olates **19** or **20** were obtained by reaction of succinonitrile with an ester R_2COOEt (R_2 = H, Me) in the presence of sodium hydride and *iso*-amyl alcohol. Treatment of **19** or **20** with phenylhydrazine or phenylhydrazine hydrochloride in the presence of triethylamine **21**-**30** in ethanol at reflux provided 2-[5-amino-1-(phenyl)-1*H*-pyrazol-4-yl]acetonitriles **31**-**43**. Compounds **31**-**43** were converted into the corresponding 5-pyrryl derivatives **44**-**56** by Klauson-Kaas[26] reaction with 2,5-dimethoxytetrahydrofuran in boiling acetic acid. Compounds **44**-**54** afforded 3-cyano-2-hydroxyacrylates **57**-**67** on treatment with diethyl oxalate in the presence of sodium ethoxide, that underwent intramolecular cyclization by heating at 90 °C in polyphosphoric acid to provide the desidered 1-(phenyl)pyrazolo[3,4-*e*]pyrrolo[3,4-*g*]indolizine-4,6(1*H*,5*H*)-diones **5**-**13**, **15** and **16**.

Scheme 1. Synthesis of Compounds 5-18.[a]

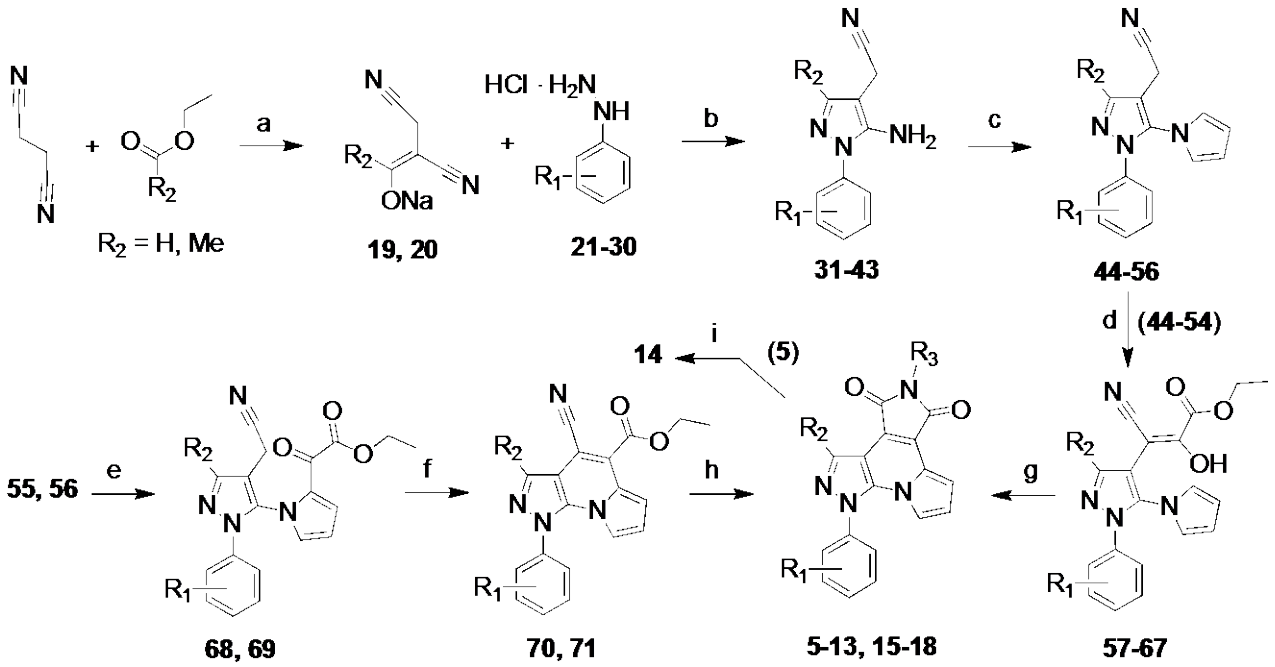

5-18, see Chart 1; **19**, R_2 = H; **20**, R_2 = Me; **21**, R_1 = H; **22**, R_1 = 2-Cl; **23**, R_1 = 3-Cl; **24**: R_1 = 4-Cl; **25**, R_1 = 2-Me; **26**, R_1 = 3-Me; **27**, R_1 = 4-Me; **28**, R_1 = 2-MeO; **29**, R_1 = 2,4-Cl_2; **30**, R_1 = 2-Me,4-Cl; **31**, **44**, **57**, R_1 = R_2 = H; **32**, **45**, **58**, R_1 = 2-Cl, R_2 = H; **33**, **46, 59**, R_1 = 3-Cl, R_2 = H; **34**, **47**, **60**, R_1 = 4-Cl, R_2 = H; **35**, **48**, **61**, R_1 = 2-Me, R_2 = H; **36**, **49**, **62**, R_1 = 3-Me, R_2 = H; **37**, **50**, **63**, R_1 = 4-Me, R_2 = H; **38**, **51**, **64**, R_1 = 2-MeO, R_2 = H; **39**, **52**, **65**, R_1 = H, R_2 = Me; **40**, **53**, **66**, R_1 = 2-Me, R_2 = Me; **41**, **54**, **67**, R_1 = 2-Cl, R_2 = Me; **42**, **55**, **68**, **70**, R_1 = 2,4-Cl_2, R_2 = Me; **43**, **56**, **69**, **71**, R_1 = 4-Cl,2-Me, R_2 = Me.

[a]*Reagents and reaction conditions:* (a) NaH, *iso*-amyl alcohol, toluene, 0 °C to room temp., 16 h; (b) ethanol, reflux, 4 h; (c) 2,5-dimethoxytetrahydrofuran, acetic acid, reflux, 30 min; (d) diethyl oxalate, sodium ethoxide, absolute ethanol, room temp., 5 h; (e) 2-chloro-2-oxoacetate, toluene, reflux, 6 h; (f) potassium carbonate, DMF, 100 °C, 4 h; (g) PPA, 90 °C, 1 h; (h) trifluoroacetic acid, sulfuric acid, room temp., 2 h; (i) potassium carbonate, DMF, room temp., 3 h.

To improve the overall yield, 2-[5-(1*H*-pyrrol-1-yl)-1-(4-methylphenyl)-1*H*-pyrazol-4-yl]acetonitriles **55** and **56** were transformed into the corresponding pyrryl-2-oxoacetates **68** and **69** with 2-chloro-2-oxoacetate in hot toluene. Intramolecular cyclization of **68** or **69** in DMF at 100 °C in the presence of potassium carbonate gave 1-(phenyl)-4-cyano-3-methyl-1*H*-pyrazolo[3,4-*e*]indolizine-5-carboxylates **70, 71** that on treatment with trifluoroacetic acid and sulfuric acid mixture furnished indolizines **17** or **18**, respectively (Scheme 1).

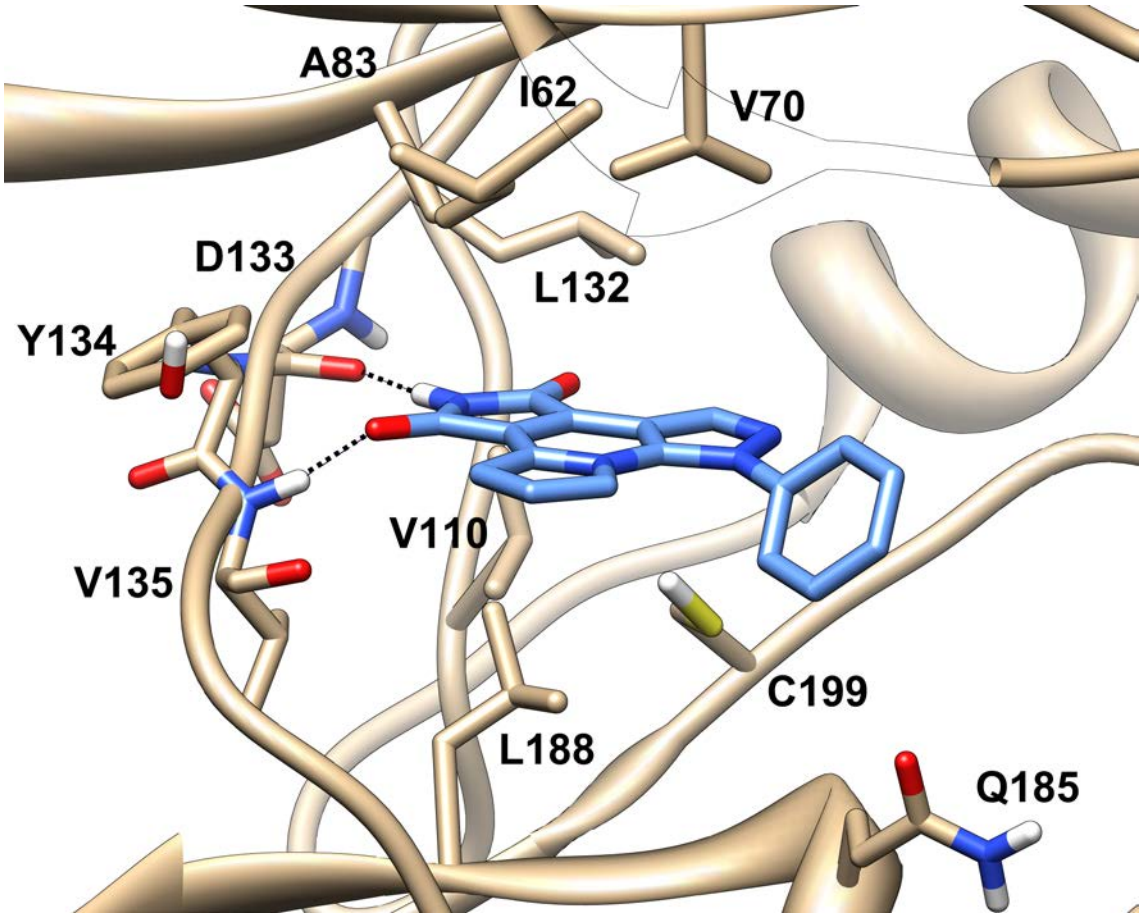

Figure 1. Binding pose of **5** in the active site of GSK-3β shown as cornflower stick and tan cartoon, respectively. Interacting residues are shown as sticks and coloured by atom type, while the H-bonds are represented by a black dashed line.

RESULTS AND DISCUSSION

Docking and MC/FEP Studies. Docking calculations of **5** into the GSK-3β active site suggested the binding pose depicted in Figure 1. Key interactions included: (i) two H-bonds established by the maleimide moiety with D133 and V135 backbone of the hinge-region; (ii) multiple hydrophobic contacts between the four planar rings and A83, V70, L132, I62 (N-lobe), L188, V110, C199, V135 (C-lobe); (iii) hydrophobic interactions of the pendant 1-phenyl ring with V70, L188, C199 and Q185 side chains.

Table 1. Computed Change in Free Energy of Binding for Introducing a Chlorine Atom or a Methyl Group at the 1-Phenyl Ring of 5.

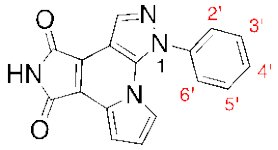

H to Cl			H to Me		
Position[a]	$\Delta\Delta G_b$[b]	σ[c]	Position[a]	$\Delta\Delta G_b$[b]	σ[c]
C2’	-0.7	0.21	C2’	-0.24	0.19
C3’	-1.1	0.18	C3’	-0.4	0.22
C4’	-1.3	0.20	C4’	-0.48	0.23
C5’	0.84	0.19	C5’	0.57	0.18
C6’	0.11	0.19	C6’	-1.754	0.18

[a]Position on the 1-phenyl ring of **5**. [b]$\Delta\Delta G_b$, computed change in free energy of binding (kcal/mol). [c]$\pm\sigma$, computed uncertainty.

Given the aforesaid binding mode, we carried out MC/FEP calculations with a chlorine and a methyl scan on the pendant 1-phenyl ring of **5** (see Table 1 for numbering). Replacement of hydrogen by chlorine was predicted to be favourable (more negative free energy of binding, $\Delta\Delta G_b$, Table 1) at C2’, C3’, and C4’ (average computed uncertainty, σ ± 0.2 kcal/mol). As for the methyl scan, a favourable replacement was predicted at C2’, C3’, C4’ and C6’ (Table 1).

Some positions were found to be equivalent, for example, both C2’ and C6’ (as it occurred for the 2’-Me analogue). When only one position was favourable (C3’-Cl and C3’-Me analogues), a penalty of RT ln 2 (0.6 kcal/mol) was due to the breakage of one rotameric state upon binding.. Thus, from the FEP scan resulted a particularly favourable replacement at C2’ or C6’, followed by C3’and the symmetrical position C4’.

Table 2. GSK3β Inhibition of Compounds 5-14 and Reference Compound 1.

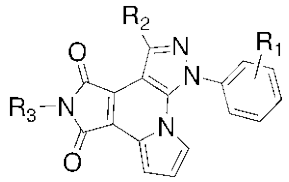

Compd	R_1	R_2	R_3	GSK-3β IC_{50} (μM)
5	H	H	H	1.69
6	2-Cl	H	H	0.81
7	3-Cl	H	H	nd
8	4-Cl	H	H	nd
9	2-Me	H	H	1.21
10	3-Me	H	H	LMR[a]
11	4-Me	H	H	LMR
12	2-OMe	H	H	1
13	H	Me	H	0.69
14	H	H	Me	nd
1	—	—	—	0.174

[a]LMR: low micromolar range.

Taking into account the synthetic accessibility of each analogue predicted to be more active than **5** by the MC/FEP calculation, a number of compounds were synthesized (Table 2). As regards the substitutions at the pendant 1-phenyl ring, the 2'-Cl (**6**) and 2'-Me (**9**) substitutions were consistent with the computed results, as compounds **6** and **9** were found potent GSK-3β inhibitors. In contrast, a discrepancy was observed for the substitutions at position 3' or 4' (**7**, **8**, **10**, **11**), which were predicted to be more active than **5**. Given the result of compound **9**, the corresponding 2'-OMe analogue (**12**) was synthesized, and it also proved to inhibit the GSK-3β.

Table 3. Computed Change in Free Energy of Binding for Introducing a Chlorine Atom or a Methyl Group at the 1-Phenyl Ring of 13.

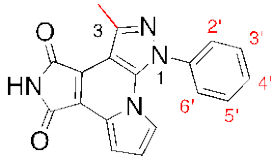

H to Cl			H to Me		
Position[a]	$\Delta\Delta G_b$[b]	σ[c]	Position[a]	$\Delta\Delta G_b$[b]	σ[c]
C2'	-2.765	0.15	C2'	-0.83	0.27
C3'	0.015	0.13	C3'	-0.731	0.21
C4'	-1.523	0.17	C4'	-1.127	0.22
C5'	1.509	0.14	C5'	0.66	0.28
C6'	-0.089	0.16	C6'	-0.059	0.29

[a]Position on the 1-phenyl ring of **13**. [b]$\Delta\Delta G_b$, computed change in free energy of binding (kcal/mol). [c]$\pm\ \sigma$, computed uncertainty.

We speculated about the replacement of the hydrogen with a chlorine or a methyl group at the position 3 of the pyrazolo[3,4-*e*]pyrrolo[3,4-*g*]indolizine-4,6(1*H*,5*H*)-dione ring. The resultant $\Delta\Delta G_b$ values were -3.8 and -2.83 kcal/mol, respectively with uncertainty of ± 0.2 kcal/mol. Consistent with the computational predictions, the introduction of a methyl group at the position 3 led to **13**, a more potent GSK-3β inhibitor than the parent compound **5**. Unfortunately, the introduction of the chlorine at this position was unsuccessful. inaccessible. We calculated the $\Delta\Delta G_b$ (6.06 kcal/mol) for the inactive methyl analogue **14**, whose prediction was in line with the experimental data.

Inspection of the complexes of **13** and **14** with the GSK-3β built using BOMB (data not shown) allows to rationalize the FEP predictions. For example, the methyl group at position 3 of **13** plunges into the *N*-lobe of the enzyme enhancing the hydrophobic contacts within the pocket. On the contrary, the introduction of a methyl group at the maleimide function of **14** disrupts the hydrogen bonds with the hinge region which are crucial for the binding process.

Table 4. Computed Change in Free Energy of Binding for Introducing Two Chlorine Atoms at the 1-Phenyl Ring of 13.

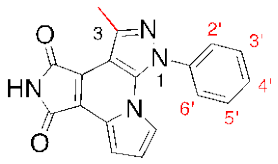

H to Cl		
Position[a]	$\Delta\Delta G_b$[b]	σ[c]
C2'/C3'	-2.765	0.21
C2'/C4'	-4.988	0.31
C2'/C5'	-1.402	0.27
C2'/C6'	-0.816	0.23
C3'/C4'	-3.026	0.27
C3'/C5'	-1.354	0.25
C3'/C6'	-1.098	0.25
C4'/C5'	0.731	0.22
C4'/C6'	-1.426	0.24
C5'/C6'	-2.541	0.22

[a]Position on the 1-phenyl ring of **13**. [b]$\Delta\Delta G_b$, computed change in free energy of binding (kcal/mol). [c]$\pm\sigma$, computed uncertainty.

A second round of MC/FEP-based optimization was attempted on the highly active compound **13**, perturbing its structure again with chlorine or methyl groups (Table 3). The replacement of hydrogen by a chlorine atom or a methyl group was predicted to be particularly favourable at C2', C4' and C6' positions. Since results for double substitutions might not be addictive, MC/FEP calculations were also accomplished for all 10 dichloro combinations, as summarized in Table 4.

Table 5. GSK3β Inhibition of Compounds 13, 15-18 and Reference Compound 1.

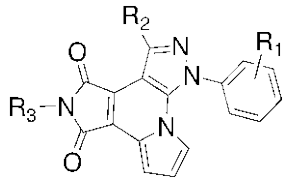

Compd	R_1	R_2	R_3	GSK-3β IC_{50} (μM)
13	H	Me	H	0.69
15	2-Me	Me	H	0.44
16	2-Cl	Me	H	0.94
17	4-Cl,2-Me	Me	H	LMR[a]
18	2,4-Cl	Me	H	0.24
1	—	—	—	0.174

[a]LMR: low micromolar range.

The results supported the viability of substitutions at C2', C3' and C4', with the most favourable substitution being C2'/C4'. Compound **15** inhibited GSK-3β with IC_{50} of 440 nM (Table 5). In line with the computational predictions, substitution at both the C2' and C4' positions with chlorine atoms led to compound **18**. It was the most potent GSK-3β inhibitor within the series, with an inhibitor activity of 240 nM, which is almost 10-fold more active than the parent compound **5**. Such an inhibitory activity was not preserved when the 2'-chlorine atom was replaced with a methyl group (compare **18** with **15** and **17**).

A picture of the computed structure for **18** bound to GSK-3β is provided in Figure 2**.** The methyl group at the C7 position is inserted in the small N-Lobe pocket where it establishes hydrophobic interactions with L132, M101, V70, and K85 side chains. As for the 1-phenyl ring, the presence of the two electron withdrawing chlorine atoms remarkably boosts the hydrophobic contacts with the aforementioned alkylic side chains of the C-lobe residues.

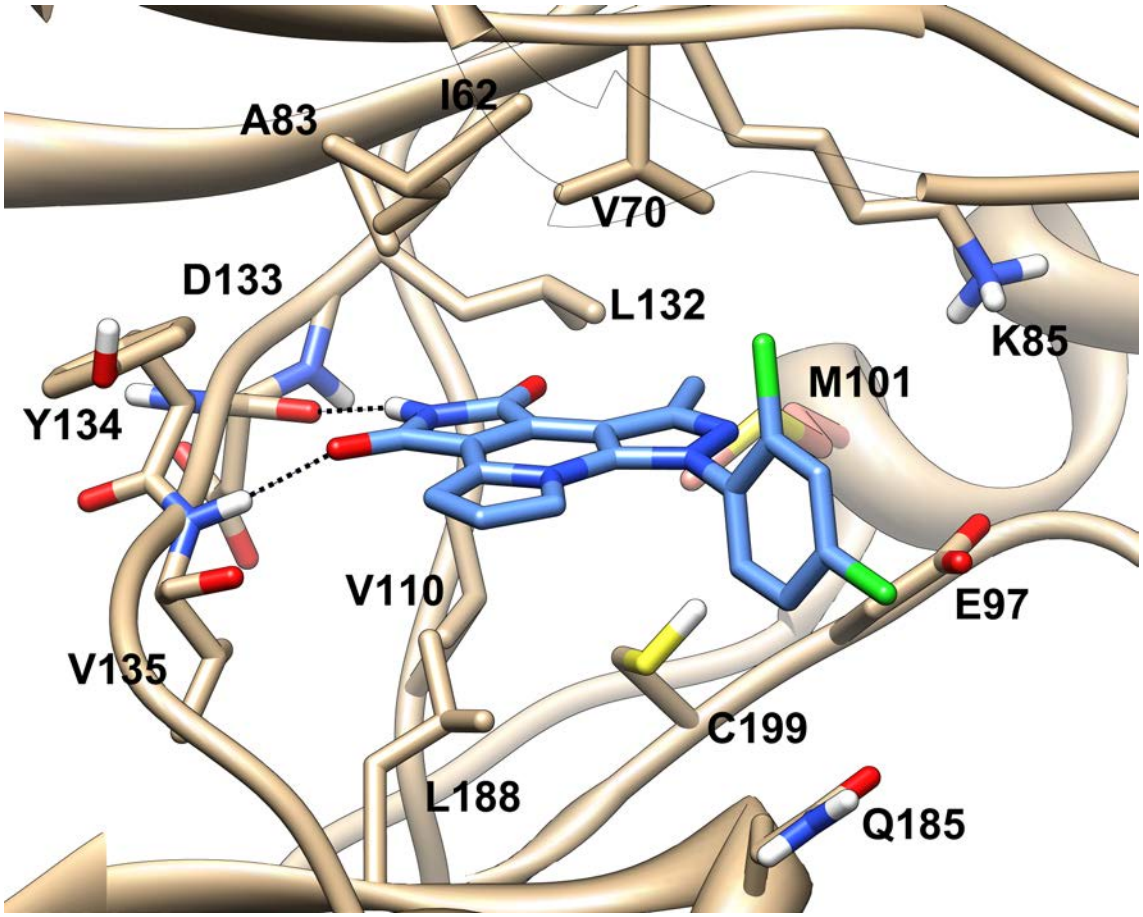

Figure 2. Putative binding pose of **18** in the active site of GSK-3β shown as cornflower stick and tan cartoon, respectively. Interacting residues are shown as sticks and colored by atom type, while the H-bond is represented by a black dashed line

Kinase Selectivity. The most potent GSK-3β inhibitor **18** was measured for the inhibition of CDK2, a proline directed Ser/Thr kinase showing high sequence similarity[27] to GSK3β in the ATP binding site. Compound **18** inhibited CDK2 with IC_{50} of 2.8 μM, and showed >10-fold selectivity.

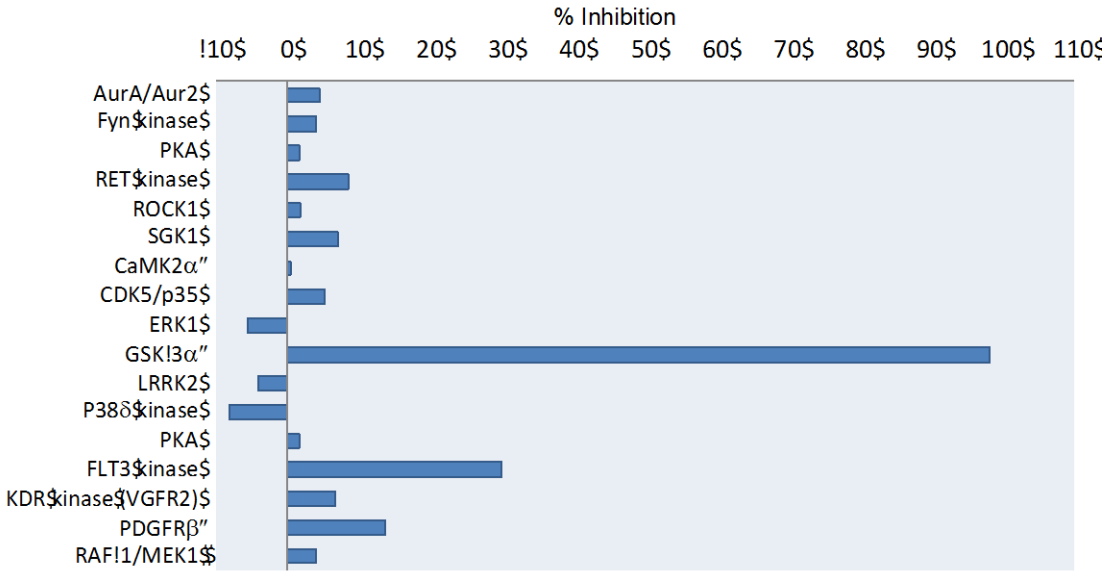

Figure 5. Histogram of % inhibition of 17 human protein kinases by compound **18**. Test concentration was 1 μM. The data represent an average of two independent measurements.

Compound **18** was tested for selectivity at a concentration of 1 μM against a panel of 17 human protein kinases selected from homologous kinases (AurA/Aur2, Fyn kinase, PKAα, RET kinase, ROCK1, SGK1), neurodegeneration kinases (CaMK2α, CDK5/p35, ERK1, GSK-3α, LRRK2, P38δ kinase, PKA), tumor kinases (FLT3 kinase, KDR kinase (VGFR2), PDGFRβ), and RAF-1/MEK1 kinase. Compound **18** displayed strong inhibition of GSK-3α□(98.3%); it weakly inhibited FLT3 kinase (30%) and PDGFRβ (13.7%), and 14 kinases of in this panel showed an inhibition lower than 10% (additional results are shown in the Supporting Information). Therefore, in summary, within this test panel compound **18** proved to be selective inhibitor of GSK-3 (Figure 5). Compound **18** was evaluated in the ovarian carcinoma cell lines OVCAR-8 and its cognate P-glycoprotein (Pgp) overexpressing line NCI/ADR-RES, and showed no activity up to 5 μM concentration in both cell lines.

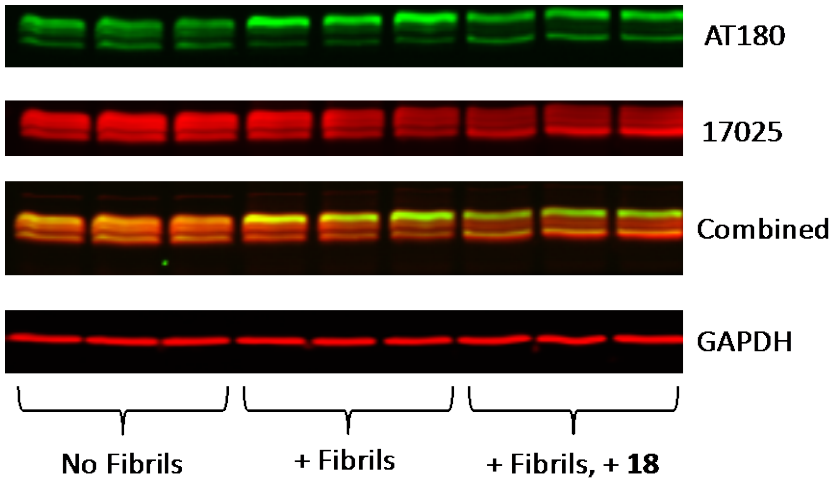

Figure 3. Compound **18** inhibits tau phosphorylation. HEK293 cells expressing human tau were treated with synthetic tau fibrils to induce the formation of intracellular tau with increased phosphorylation. This can be seen by an increase in the slower migrating species of tau using the AT180 antibody that recognizes the p231T and p235S phospho-epitopes of tau. Treatment with 1 μM **18** led to decrease in the slow mobility AT180 band and an increase in the faster migrating AT180 band, as well as an increase in the higher mobility band recognized by the 17025 antibody to total tau. The combined gel is a composite of the AT180 and 17025 immunoreactivity, and GAPDH is glyceraldehydes 3-phosphate dehydrogenase, which is utilized as a housekeeping protein to demonstrate equal protein loading.

Inhibition of Protein Tau Phosphorylation. To investigate the ability of this class of compounds to modulate the phosphorylation state of a known GSK3β substrate in a cell-based assay, we evaluated a representative example, **18**, in a HEK-293 cell model in which the full-length four-repeat tau isoform (T40), bearing the P301L mutation (T40PL) found in a form of inherited frontotemporal dementia[28,29] is expressed under the control of a doxycycline-regulated promoter.

Such cells can be induced to form intracellular inclusions of misfolded tau that bear resemblance to the hyperphosphorylated NFTs observed in Alzheimer's disease and related tauopathies, if the cells are "seeded" with small amounts of synthetic tau fibrils that are created from recombinant tau protein.[30] Here, the HEK-293 cells were treated with doxycycline to induce tau expression, and 48 h later were treated with synthetic tau fibrils, followed by treatment with **18** or vehicle for an additional

48 h. Non-fibril treated tau-expressing cells were included as controls. GSK-3β, as well as other kinases, can phosphorylate tau at residues T231 and S235,[31] the extent of tau phosphorylation at these sites was examined by immunoblot analysis of the cell lysates, employing the AT180 antibody which recognizes the tau pT231 and pS235 epitopes. In addition, total tau was examined by immunoblotting with the polyclonal 17025 antibody to full-length tau.

The total tau immunoblot reveals multiple tau species with slightly differing electrophoretic mobilities (Figure 3; 17025). As a single isoform of tau is expressed in these cells, the multiple bands presumably represent tau with different charges that result from post-translational modifications, such as phosphorylation. In fact, all of the AT180-positive species (Figure 3; AT180) co-migrate with tau (Figure 3; combined).

Relative to cells that were not seeded with fibrils, the AT180 signal is increased in the slowest migrating tau species and faster migrating bands are decreased after tau fibril treatment (Figure 3 and Figure 4-A), with the total AT180 signal remaining unchanged in the fibril-treated cells compared to non-fibril cells (Figure 4-B). This would suggest that the fibril treatment resulted in increased phosphorylation at tau residues other than T231 or S235. Interestingly, addition of **18** to the fibril-treated cells resulted in a diminution of the slowest migrating and an increase in the faster migrating AT180 species (Figure 3 and Figure 4-A). A somewhat similar shift in distribution can be seen in the 17025 immunoblot of total tau after treatment of the fibril-seeded cells with **18**, with an increase in the percentage of tau with faster electrophoretic mobility relative to the vehicle-treated cells (Figure 3 and Figure 4-C). As expected, there was no significant difference in the amount of total tau in the different treatment conditions (Figure 4-D). Taken in totality, these data suggest that **18** inhibited tau phosphorylation, but at a site(s) other than the pT231 and pS235 sites that are recognized by the AT180 antibody.

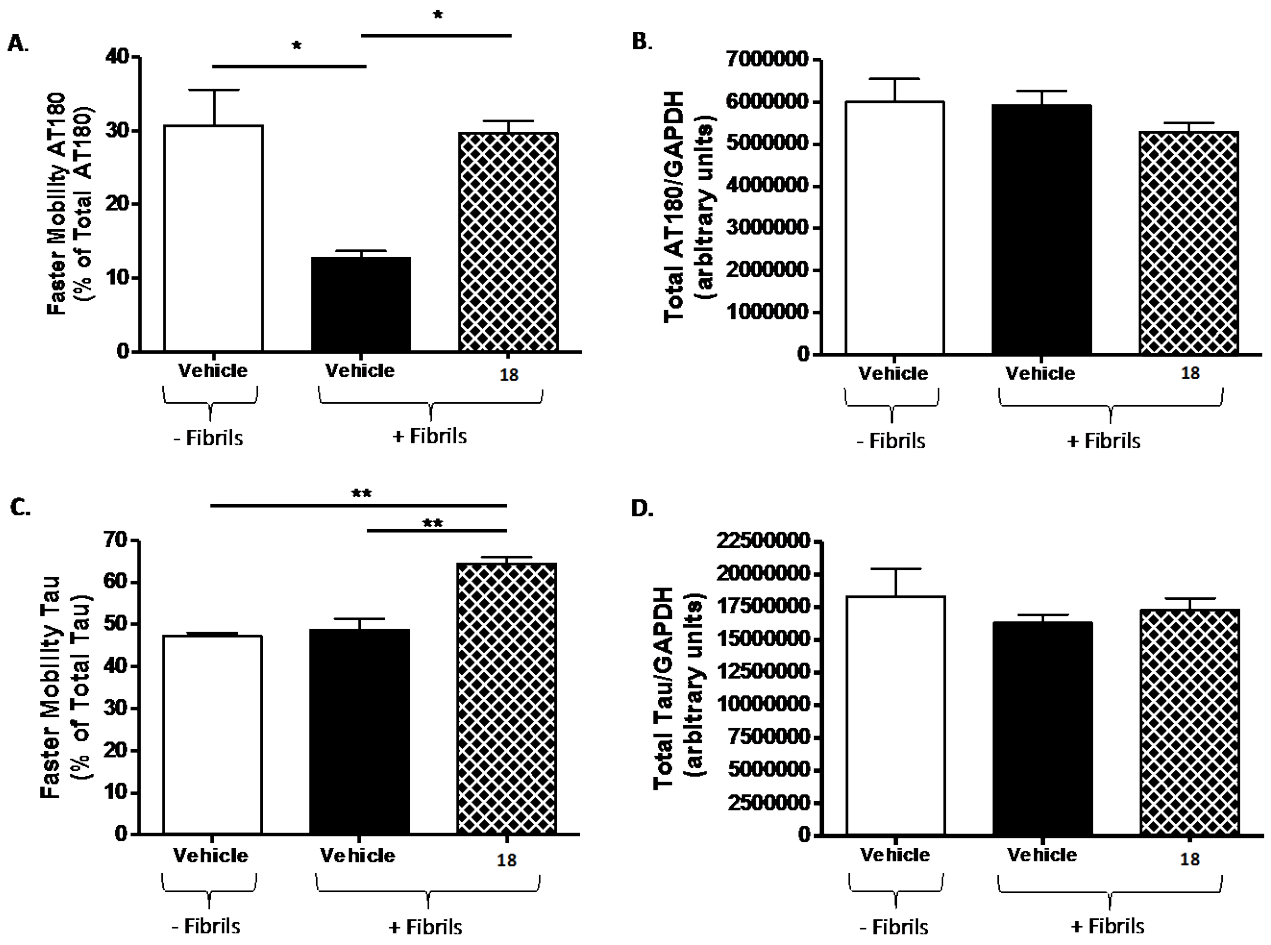

Figure 4. Quantification of the high mobility AT180- and 17025-positive tau species in Figure 3. The fastest migrating AT180 and 17025 immunoreactive species shown in Figure 3 were quantified as described in the Methods. In addition, the combined AT180 and 17025 immunoreactive species were quantified and normalized to the housekeeping protein, GAPDH.

GSK-3β is known to phosphorylate tau at sites other than T231/S235, including S202 and S396,[31] and thus the altered electrophoretic profile of tau after **18** treatment may have resulted from inhibition of phosphorylation at one or both of these residues. It is somewhat surprising that **18** did not cause a reduction in total AT180 immunostaining, since this antibody recognizes known GSK-3β phosphorylation sites. However, other kinases can also phosphorylate T231 and S235 of tau,[31] and thus it is possible that one or more of these kinases acts on these residues in the HEK-293 cells, rather than GSK-3β.

Evaluation of predicted physico-chemical properties and blood-brain barrier permeability. To achieve optimum therapeutic efficacy, a GSK-3β inhibitor should display suitable physico-chemical properties for CNS penetration. Most of the early predictive models for BBB penetration are based on a multiple linear regression approach and combination of three or more descriptors, i.e. the calculated LogP, the number of H-bond acceptors in an aqueous medium and the polar surface area.[32.33] In our design strategy, a qualitative prediction of the physico-chemical properties of all the analogues generated for the MC/FEP calculations has been automatically perfomed by the BOMB program using the Qikprop software (Schrödinger, LLC New York). These preliminary data suggested that our ligands have the potential to passively diffuse across the BBB. We herein report the computed physico-chemical properties of **5** and **18.**

These measurements suggested that compound **18**, the most potent GSK-3β inhibitor within the series, exhibited properties that should favour CNS penetration,[32.33] including: (i) a molecular weight <400 Da; (ii) a log P value comprised between 0 and 5; (iii) less than 3 H-bond donors; (iv) less than 7 H-bond acceptor, (v) the number of rotatable bonds comprised between 0 and 5; (vi) log BB value comprised between -3 and 1; and (vii) the PSA <90 $Å^2$ (Table 6).

Table 6. Calculated physico-chemical properties of 5 and 18 performed by the Qikprop software

Compd	MW	log P (o/W)	HB donor	HB acceptor	# rotor	logBB	PSA
5	302	2.5	1	4	0	-0.612	94
18	371	3.4	1	4	0	-0.283	87.47

The BBB permeation profiles of our synthesized compounds were also predicted a posteriori using the BBB VolSurf model, whereby a variety of 3D molecular field descriptors were transformed into a

new set of descriptors to produce a model by using a discriminant partial least squares (PLS) procedure.[34,35] All our compounds were built in 3D coordinates and then projected in the VolSurf Crivori model.[34] This model was able to discriminate between penetrating (BBB+) and non-penetrating (BBB–) compounds. Figure 1S of Supporting Infomation shows the BBB profile as predicted by VolSurf. All of our molecules were located in the BBB+ region of the plot with the exception of **5** which is in the borderline region.

Aqueous Solubility. The solubility in aqueous pH 7.4 buffer of compound **18** was measured by Cerep. Compound **18** showed to be moderately soluble in water, with mean solubility of 3.1 μM (additional results are shown in the Supporting Information).

CONCLUSION

In search for agents to treat neurodegenerative diseases, GSK-3β inhibitors have become an attractive target as growing evidence correlates an increase in GSK-3β activity with neurodegeneration. Compound **5** from our in-house library was selected as a suitable starting point for the rational design of new GSK-3β inhibitors. MC/FEP calculations of **5** led to the identification of a structural class of new GSK-3β inhibitors. Compound **18** inhibited GSK-3β with IC_{50} of 0.24 μM, and it was found to be a selective inhibitor of GSK-3 against a panel of 17 kinases, with >10-fold selectivity against CDK2. Furthermore, **18** inhibited tau phosphorylation in a cell-based assay. Finally, calculation of physico-chemical properties suggested that compound **18** exhibits properties that favour passive diffusion across the BBB In summary, we have developed a new class of GSK-3β inhibitors. Compound **18**

represents a robust lead compound to develop GSK-3β inhibitors with improved activity and selectivity that have potential as novel therapeutic agents to treat neurodegenerative disorders.

EXPERIMENTAL SECTION

Chemistry. All reagents and solvents are commercially available and were used as purchased, without further purification. Melting points (mp) were determined on a Stuart Scientific SMP1 apparatus and are uncorrected. Infrared spectra (IR) were run on a Perkin-Elmer SpectrumOne FT-ATR spectrophotometer. Band position and absorption ranges are given in cm^{-1}. Proton nuclear magnetic resonance (^1H NMR) spectra were recorded on a Bruker 400 MHz FT spectrometer in the indicated solvent and corresponding fid files processed by MestreLab Research S.L. MestreReNova 6.2.1-769 software. Chemical shifts are expressed in δ units (ppm) from tetramethylsilane. Column chromatography was performed on columns packed with alumina from Merck (70−230 mesh) or silica gel from Macherey-Nagel (70-230 mesh). Aluminum oxide thin layer chromatography (TLC) cards from Fluka (aluminum oxide precoated aluminum cards with fluorescent indicator detectable at 254 nm) and silica gel TLC cards from Macherey-Nagel (silica gel precoated aluminum cards with fluorescent indicator detectable at 254 nm) were used for TLC. Developed plates were visualized by a Spectroline ENF 260C/FE UV apparatus. Organic solutions were dried over anhydrous sodium sulfate. Evaporation of the solvents was carried out on a Büchi rotavapor R-210 equipped with a Büchi V-855 vacuum controller and a Büchi V-700 or V-710 vacuum pump. Elemental analyses of the compounds were found within ±0.4% of the theoretical values. The purity of tested compounds was >95%. Phenylhydrazines purchased from commercial sources (Scheme 1): **21**, R_1 = H; **22**, R_1 = 2-Cl; **23**, R_1 = 3-Cl; **24**, R_1 = 4-Cl; **25**, R_1 = 2-Me; **26**, R_1 = 3-Me; **27**, R_1 = 4-Me; **28**, R_1 = 2-OMe; **29**, R_1 = 2,4-Cl_2; **30**, R_1 = 2-Me,4-Cl.

General procedure for the synthesis of derivatives 5-13, **15 and 16**. **Example. 1-(4'-Methylphenyl)pyrazolo[3,4-*e*]pyrrolo[3,4-*g*]indolizine-4,6(1*H*,5*H*)-dione (11)**. Compound **63** (2.18 g, 0.006 mol) was added in small portions to polyphosphoric acid (PPA) (22 g) pre-heated at 90 °C. The reaction mixture was stirred at 90 °C for 1 h and then allowed to cool at room temperature. Water was carefully added (exotermal reaction!) and the mixture was extracted with ethyl acetate. The combined organic layers were washed with brine and dried, and the solvent was evaporated. The residue was purified by silica gel column chromatography using ethyl acetate:*n*-hexane (1:1) as eluent to give **11** (0.70 g, yield 37%), mp 234-237 °C (from aqueous ethanol). ^{1}H NMR (DMSO-d_6)□δ 11.09 (s, 1H), 8.36 (d, *J* = 3.0 Hz, 1H), 7.60 (m, 2H), 7.50 (d, *J* = 8.0 Hz, 2H), 7.09 (dd, *J* = 1.1 and 4.0 Hz, 1H), 6.93 (dd, *J* = 2.9 and 4.0 Hz, 1H), 6.85 (dd, *J* = 1.1 and 2.9 Hz, 1H), 2.48 ppm (s, 3H). IR□ ν 1711, 1759, 3199 cm^{-1}. Anal. Calcd. for $C_{18}H_{12}N_4O_2$ (316.31), C, H, N

1-Phenylpyrazolo[3,4-*e*]pyrrolo[3,4-*g*]indolizine-4,6(1*H*,5*H*)-dione (5). Was prepared as **11** from **57**.[20]

1-(2'-Chlorophenyl)pyrazolo[3,4-*e*]pyrrolo[3,4-*g*]indolizine-4,6(1*H*,5*H*)-dione (6). Was prepared as **11** from **58**. Yield 46%, mp 230-232 °C (from aqueous ethanol). ^{1}H NMR (DMSO-d_6)□δ 8.48 (s, 1H), 8.32 (s, 1H), 7.95 (dd, *J* = 7.8, 1.5 Hz, 1H), 7.89 (dd, *J* = 8.1 and 1.3 Hz, 1H), 7.82 (d, *J* = 1.6 Hz, 1H), 7.73 (dd, *J* = 7.6 and 1.4 Hz, 1H), 7.14-7.10 (m, 1H), 7.00-6.92 (m, 1H), 6.72 – 6.67 ppm (m, 1H). IR□ν 1707, 1758, 2726, 3034, 3149 cm^{-1}. Anal. Calcd. for $C_{17}H_9ClN_4O_2$ (336.73), C, H, N, Cl.

1-(3'-Chlorophenyl)pyrazolo[3,4-*e*]pyrrolo[3,4-*g*]indolizine-4,6(1*H*,5*H*)-dione (7). Was prepared as **11** from **59**. Yield 49%, mp 288-290 °C (from aqueous ethanol). ^{1}H NMR (DMSO-d_6)□δ 11.14 (s, 1H), 8.41 (s, 1H), 7.92 (s, 1H), 7.78 (m, 3H), 7.12 (m, 1H), 7.98 (m, 1H), 6.94 ppm (m, 1H). IR□ ν 1727, 17645, 3235 cm^{-1}. Anal. Calcd. for $C_{17}H_9ClN_4O_2$ (336.73), C, H, N, Cl.

1-(4'-Chlorophenyl)pyrazolo[3,4-*e*]pyrrolo[3,4-*g*]indolizine-4,6(1*H*,5*H*)-dione (8). Was prepared as **11** from **60.** Yield 61%, mp 279-281 °C (from aqueous ethanol). ^{1}H NMR (DMSO-d_6): δ 11.10 (s,

1H), 8.40 (s, 1H), 7.77 (s, 4H), 7.12 (m, 1H), 6.96 ppm (m, 2H). IR□ν 1721, 1759, 3240 cm^{-1}. Anal. Calcd. for $C_{17}H_9ClN_4O_2$ (336.73), C, H, N, Cl.

1-(2'-Methylphenyl)pyrazolo[3,4-*e*]pyrrolo[3,4-*g*]indolizine-4,6(1*H*,5*H*)-dione (9). Was prepared as **11** from **61**. Yield 40%, mp 227-231 °C (from aqueous ethanol). ^{1}H NMR (DMSO-d_6): δ 11.11 (s, 1H), 8.44 (s, 1H), 7.63 (m, 3H), 7.53 (t, J = 7.4 Hz, 1H), 7.10 (m, 1H), 6.90 (m, 1H), 6.60 (m, 1H), 1.95 ppm (s, 3H). IR: ν 1713 cm^{-1}. Anal. Calcd. for $C_{18}H_{12}N_4O_2$ (316.31), C, H, N.

1-(3'-Methylphenyl)pyrazolo[3,4-*e*]pyrrolo[3,4-*g*]indolizine-4,6(1*H*,5*H*)-dione (10). Was prepared as **16** from **62**. Yield 57%, mp 232-234 °C (from ethyl acetate-*n*-hexane). ^{1}H NMR (DMSO-d_6): δ 11.09 (s, 1H), 8.39 (s, 1H), 7.55 (m, 4H), 7.12 (m, 1H), 6.94 (m, 1H), 6.88 (m, 1H), 2.45 ppm (s, 3H). IR: ν 1720, 1758, 1832, 3061, 3171, 3227 cm^{-1}. Anal. Calcd. for $C_{18}H_{12}N_4O_2$ (316.31), C, H, N.

1-(2'-Methoxyphenyl)pyrazolo[3,4-*e*]pyrrolo[3,4-*g*]indolizine-4,6(1*H*,5*H*)-dione (12). Was prepared as **11** from **64**. Yield 27%, mp 282-284 °C (from aqueous ethanol). ^{1}H NMR (DMSO-d_6): δ 11.04 (s, 1H), 8.37 (s, 1H), 7.70 (m, 2H), 7.38 (d, *J* = 8.2 Hz, 1H), 7.24 (t, *J* = 7.6 Hz, 1H), 7.08 (m, 1H), 6.92 (m, 1H), 6.81 (m, 1H), 3.65 ppm (s, 3H). IR: ν 1720, 1756, 3154 cm^{-1}. Anal. Calcd. for $C_{18}H_{12}N_4O_3$ (332.31), C, H, N.

3-Methyl-1-phenylpyrazolo[3,4-*e*]pyrrolo[3,4-*g*]indolizine-4,6(1*H*,5*H*)-dione (13). Was prepared as **11** from **65**. Yield 52%, mp >270 °C (from ethanol). ^{1}H NMR (DMSO-d_6): δ 11.06 (s, 1H), 7.69 (m, 5H), 7.07 (dd, *J* = 1.0 and 4.0 Hz, 1H), 6.91 (dd, *J* = 3.0 and 4.0 Hz, 1H), 6.77 (dd, *J* = 1.0 and 2.9 Hz, 1H), 2.72 ppm (s, 3H). IR: ν 1724, 1754, 2735, 3062, 3265, 3482 cm^{-1}. Anal. Calcd. for $C_{18}H_{12}N_4O_2$ (316.31), C, H, N.

3-Methyl-1-(2'-methylphenyl)pyrazolo[3,4-*e*]pyrrolo[3,4-*g*]indolizine-4,6(1*H*,5*H*)-dione (15). Was prepared as **11** from **66**. Yield 19%, mp 227-231 °C (from aqueous ethanol). ^{1}H NMR (DMSO-d_6): δ 11.04 (s, 1H), 7.50 (m, 4H), 7.07 (m, 1H), 6.89 (m, 1H), 6.55 (m, 1H), 2.75 (s, 3H), 1.96 ppm (s, 3H). IR: ν 1718, 1761, 2722, 3069, 3182 cm^{-1}. Anal. Calcd. for $C_{19}H_{14}N_4O_2$ (330.34), C, H, N.

3-Methyl-1-(2'-chlorophenyl)pyrazolo[3,4-*e*]pyrrolo[3,4-*g*]indolizine-4,6(1*H*,5*H*)-dione (16). Was prepared as **11** from **67**. Yield 67%, mp 200-204 °C (from aqueous ethanol). ^{1}H NMR (DMSO-d_6): δ 11.11 (s, 1H), 7.91 (d, *J* = 6.3 Hz, 1H), 7.86 (d, *J* = 8.0 Hz, 1H), 7.79 (t, *J* = 7.0 Hz, 1H), 7.69 (t, *J* = 7.6 Hz, 1H), 7.10 (m, 1H), 6.94 (m, 1H), 6.65 (m, 1H), 2.75 ppm (s, 3H). IR: ν 1707, 1761, 3169 cm^{-1}. Anal. Calcd. for $C_{18}H_{11}ClN_4O_2$ (350.76), C, H, N, Cl.

General procedure for the synthesis of derivatives 17 and 18. 1-(4'-Chloro-2'-methylphenyl)-3-methylpyrazolo[3,4-*e*]pyrrolo[3,4-*g*]indolizine-4,6(1*H*,5*H*)-dione (17). A solution of **71** (0.0105 g, 0.00026 mol), trifluoroacetic acid (0.24 mL) and sulfuric acid (0.12 mL) was stirred at room temperature for 2 h. Water was carefully added dropwise (exotermic reaction!) and the mixture was extracted with ethyl acetate, washed with brine and dried. After evaporation of the solvent, the residue was purified by silica gel column chromatography using ethyl acetate:*n*-hexane (1:2) as eluent to obtain **18** (0.03 g, yield 31%), mp 230-233 °C (from aqueous ethanol). ^{1}H NMR (DMSO-d_6): δ 11.07 (s, 1H), 7.69 (s, 1H), 7.63 (d, *J* = 8.4 Hz, 1H), 7.56 (d, *J* = 10.4 Hz, 1H), 7.08 (d, *J* = 3.9 Hz, 1H), 6.93 – 6.90 (m, 1H), 6.67 (d, *J* = 2.5 Hz, 1H), 2.73 (s, 3H), 1.96 ppm (s, 3H). IR: ν 1712, 1765, 3122, 3293 cm^{-1}. Anal. Calcd. for $C_{19}H_{13}ClN_4O_2$ (364.79), C, H, N, Cl.

1-(2',4'-Dichlorophenyl)-3-methylpyrazolo[3,4-e]pyrrolo[3,4-g]indolizine-4,6(1*H*,5*H*)-dione (18). Was prepared as **18** from **70**. Yield 29%, mp 236-240 °C (from ethanol). ^{1}H NMR (DMSO-d_6): δ 11.08 (s, 1H), 8.06 (d, *J* = 2.2 Hz, 1H), 7.93 (d, *J* = 8.5 Hz, 1H), 7.77 (dd, *J* = 2.3 and 8.5 Hz, 1H), 7.09 (m, 1H), 6.94 (m, 1H), 6.80 (m, 1H), 2.73 ppm (s, 3H). IR: ν 1708, 1765, 3094 cm^{-1}. Anal. Calcd. for $C_{18}H_{10}Cl_2N_4O_2$ (385.20), C, H, N, Cl.

5-Methy-1-Phenylpyrazolo[3,4-*e*]pyrrolo[3,4-*g*]indolizine-4,6(1*H*,5*H*)-dione (14). A mixture of **5** (0.3 g, 0.001 mol), methyl iodide (0.17 g, 0.0012 mol) and potassium carbonate (0.21 g, 0.0015 mol) in DMF (5 mL) was stirred at room temperature for 3 h. After dilution with water, the mixture was extracted with ethyl acetate, washed with brine and dried. Evaporation of the solvent gave a residue

that was purified by silica gel column chromatography using ethyl acetate:*n*-hexane (1:2) as eluent to obtain **14** (0.26 g, yield 85%). mp 217-221 °C (from ethanol). ^{1}H NMR (DMSO-d_6): δ 3.05 (s, 3H), 6.85 (d, J = 2.0 Hz, 1H), 6.95 (t, J = 3.0 Hz, 1H), 7.11 (d, J = 3.1 Hz, 1H), 7.72-74 (m, 5H), 8.41 ppm (s, 1H). Anal. Calcd. for $C_{18}H_{12}N_4O_2$ (316.31), C, H, N.

Sodium 2,3-dicyanoprop-1-en-1-olate (19). A suspension of NaH (60 % dispersion in mineral oil, 0.48 g, 0.012 mol) and *iso*-amyl alcohol (0.2 mL) in anhydrous toluene (10 mL) was heated at reflux for 30 min. After cooling at room temperature, a solution of succinonitrile (0.80 g, 0.01 mol) and ethyl formiate (7.79 g, 8.5 mL, 0.105 mol) in anhydrous toluene (5 mL) was added dropwise. The reaction mixture was stirred at room temperature overnight. The solid product was collected to provide the desired compound **19** as a solid (1.2 g, yield 77%), mp 180 °C (dec.). ^{1}H NMR (DMSO-d_6): δ δ 8.5 (s, 1H), 2.91ppm (s, 2H) ppm. IR: ν 2181, 2246, 3376 cm^{-1}.

Sodium 3,4-dicyanobut-2-en-2-olate (20). Was prepared as **44** using ethyl acetate. Yield 95%, mp 217-221 °C. ^{1}H NMR (DMSO-d_6): δ 3.68 (s, 2H), 2.04 ppm (s, 3H). IR: ν 2161, 2255, 3349 cm^{-1}.

General procedure for the synthesis of derivatives 31-43. Example. 2-[5-Amino-1-(4'-methylphenyl)-1*H*-pyrazol-4-yl]acetonitrile (37). A mixture of **19** (3.00 g, 0.023 mol), 4-methylphenylhydrazine hydrochloride (**27**) (4.38 g, 0.028 mol) in ethanol (23 mL) was heated at reflux for 2 h. After cooling, the solvent was evaporated and water was added. The mixture was extracted with ethyl acetate. The combined organic layers were washed with brine and dried. The crude residue was purified by silica gel column chromatography using dichloromethane as eluent to give **37** (2.7 g, yield 56%), mp 115-119 °C (from from aqueous ethanol). ^{1}H NMR ($CDCl_3$): δ 7.40 – 7.32 (m, 3H), 7.28 (d, *J* = 8.1 Hz, 2H), 3.96 (s, 2H), 3.47 (s, 2H), 2.40 ppm (s, 3H). IR: ν 2252, 3152, 3376 cm^{-1}.

2-[5-Amino-1-(phenyl)-1*H*-pyrazol-4-yl]acetonitrile (31). Was prepared as **37** from **19** and phenylhydrazine.[20]

2-[5-Amino-1-(2'-chlorophenyl)-1*H*-pyrazol-4-yl]acetonitrile (32). Was prepared as **37** from **19**,

2-chlorophenylhydrazine hydrochloride and triethylamine. Yield 54%, mp 98-100 °C (from aqueous ethanol). ^{1}H NMR (DMSO-d_6): δ 7.66 (dd, J = 7.8, 1.5 Hz, 1H), 7.52 (dd, J = 9.5 and 1.8 Hz, 2H), 7.48 – 7.42 (m, 1H), 7.34 (s, 1H), 5.28 (s, 2H), 3.67 ppm (s, 2H). IR: ν 2247, 3199, 3315, 3382 cm^{-1}.

2-[5-Amino-1-(3'-chlorophenyl)-1*H*-pyrazol-4-yl]acetonitrile (33). Was prepared as **37** from **19** and 3-chlorophenylhydrazine hydrochloride. Yield 28%, mp 144-146 °C (from toluene). ^{1}H NMR ($CDCl_3$): δ 7.70 (t, J = 1.9 Hz, 1H), 7.60 – 7.53 (m, 2H), 7.46 (t, J = 8.0 Hz, 1H), 7.40 – 7.34 (m, 1H), 3.99 (s, 2H), 1.58 ppm (s, 2H). IR: ν 3091, 3315, 3400 cm^{-1}.

2-[5-Amino-1-(4'-chlorophenyl)-1*H*-pyrazol-4-yl]acetonitrile (34). Was prepared as **37** from **19** and 4-chlorophenylhydrazine hydrochloride. Yield 42% as an oil. ^{1}H NMR (DMSO-d_6): δ 7.61 (d, J = 8.8 Hz, 2H), 7.55 (d, J = 8.9 Hz, 2H), 7.39 (s, 1H), 5.51 (s, 2H), 3.69 ppm (s, 2H). IR: ν 2255, 3154, 3369 cm^{-1}.

2-[5-Amino-1-(2'-methylphenyl)-1*H*-pyrazol-4-yl]acetonitrile (35). Was prepared as **37** from **19** and 2-methylphenylhydrazine hydrochloride. Yield 87% as an oil. ^{1}H NMR (DMSO-d_6): δ 7.44 – 7.37 (m, 2H), 7.35 – 7.30 (m, 2H), 7.24 (d, J = 7.5 Hz, 1H), 5.16 (s, 2H), 3.68 (s, 2H), 2.04 ppm (s, 3H). IR: ν 2248, 3196, 3324 cm^{-1}.

2-[5-Amino-1-(3'-methylphenyl)-1*H*-pyrazol-4-yl]acetonitrile (36). Was prepared as **37** from **19** and 3-methylphenylhydrazine hydrochloride. Yield 37% as an oil. ^{1}H NMR (DMSO-d_6): δ 7.46 – 7.26 (m, 4H), 7.25 – 7.09 (m, 1H), 5.44 (s, 2H), 3.69 (s, 2H), 2.37 ppm (s, 3H). IR: ν 2248, 3197, 3330 cm^{-1}.

2-[5-Amino-1-(2'-methoxyphenyl)-1*H*-pyrazol-4-yl]acetonitrile (38). Was prepared as **37** from **19** and 2-methoxyphenylhydrazine hydrochloride. Yield 10% an an oil. ^{1}H NMR ($CDCl_3$): δ 7.45 (d, J = 3.2 Hz, 1H), 7.45 – 7.40 (m, 2H), 7.13 – 7.06 (m, 2H), 3.88 (s, 2H), 3.80 (s, 1H), 3.53 ppm (s, 2H). IR: ν 2247, 2938, 3331 cm^{-1}.

2-[5-Amino-3-methyl-1-(phenyl)-1*H*-pyrazol-4-yl]acetonitrile (39). Was prepared as **37** from **20**

and phenylhydrazine hydrochloride. Yield 71%, mp 137-140 °C (from aqueous ethanol). ^{1}H NMR (DMSO-d_6): δ 7.55 (d, J = 7.5 Hz, 2H), 7.47 (t, J = 7.9 Hz, 2H), 7.31 (t, J = 7.3 Hz, 1H), 5.42 (s, 2H), 3.68 (s, 2H), 2.11 ppm (s, 3H). IR: ν 2245, 3175, 3281, 3425 cm^{-1}.

2-[5-Amino-3-methyl-1-(2'-methylphenyl)-1*H*-pyrazol-4-yl]acetonitrile (40). Was prepared as **37** from **20** and 2-methylphenylhydrazine hydrochloride. It was used as a crude compound.

2-[5-Amino-1-(2'-chlorophenyl)-3-methyl-1*H*-pyrazol-4-yl])acetonitrile (41). Was prepared as **37** from **20** and 2-chlorophenylhydrazine. Yield 51%, mp 140-142 °C (from aqueous ethanol). ^{1}H NMR (DMSO-d_6) ^{1}H NMR (DMSO-d_6): δ 7.64 – 7.60 (m, 1H), 7.52 – 7.39 (m, 3H), 5.22 (s, 2H), 3.64 (s, 2H), 2.08 ppm (s, 3H). IR: ν 3155 cm^{-1}.

2-(5-Amino-1-(2',4'-dichlorophenyl)-3-methyl-1*H*-pyrazol-4-yl)acetonitrile (42). Was prepared as **37** from **20** and 2,4-dichlorophenylhydrazine hydrochloride. Yield 73%, mp 96-98 °C (from aqueous ethanol). ^{1}H NMR (DMSO-d_6): δ 7.80 (d, J = 2.3 Hz, 1H), 7.53 (dd, J = 8.5, 2.3 Hz, 1H), 7.44 (d, J = 8.5 Hz, 1H), 5.34 (s, 2H), 3.63 (s, 2H), 2.07 ppm (s, 3H). IR: ν 2248, 3158, 3282, 3398 cm^{-1}.

2-[5-Amino-1-(4'-chloro-2'-methylphenyl)-3-methyl-1*H*-pyrazol-4-yl]acetonitrile (43). Was prepared as **37** from **20** and 4-chloro-2-methylphenylhydrazine hydrochloride. Yield 28% as an oil. ^{1}H NMR (DMSO-d_6): δ 7.45 (s, 1H), 7.34 (d, J = 8.7 Hz, 1H), 7.23 (d, J = 8.5 Hz, 1H), 5.20 (s, 2H), 3.63 (s, 2H), 2.07 (s, 3H), 2.04 ppm (s, 3H). IR: ν 2240, 3127, 3392 cm^{-1}.

General procedure for the synthesis of derivatives 44-56. Example. 2-(1-(4'-Methylphenyl)-5-(1*H*-pyrrol-1-yl)-1*H*-pyrazol-4-yl)acetonitrile (50). A mixture of **37** (2.50 g, 0.0118 mol) and 2,5-dimethoxytetrahydrofuran (1.62 g, 1.59 mL, 0.0123 mol) in acetic acid (12 mL) was heated at reflux for 30 min. After cooling, the solvent was removed, and the residue was dissolved in water and extracted with ethyl acetate. The combined organic layers were washed with a solution of sodium hydrogen carbonate, brine and dried. Removal of the solvent gave a residue that was purified by silica gel column chromatography using ethyl acetate:*n*-hexane 1:3 as eluent to obtain **50** (2.0 g, yield 64%),

mp 74-79 °C (from *n*-hexane). ^{1}H NMR (DMSO-d_6): δ 7.85 (s, 1H), 7.17 (d, *J* = 8.7 Hz, 2H), 6.99 (d, *J* = 8.4 Hz, 2H), 6.90 – 6.80 (m, 2H), 6.33 – 6.23 (m, 2H), 3.82 – 3.72 (m, 2H), 2.30 ppm (s, 3H). IR: ν 2252, 3121 cm^{-1}.

2-[1-Phenyl-5-(1*H*-pyrrol-1-yl)-1*H*-pyrazol-4-yl]acetonitrile (44). Was prepared as **50** from **31**.[20]

2-(1-(2'-Chlorophenyl)-5-(1*H*-pyrrol-1-yl)-1*H*-pyrazol-4-yl)acetonitrile (45). Was prepared as **50** from **32**. Yield 86% as an oil. ^{1}H (DMSO-d_6): δ 7.89 (s, 1H), 7.6 (m, 2H), 7.51 (m, 1H), 7.44 (m, 1H), 6.79 (m, 2H), 6.16 (m, 2H), 3.83 ppm (s, 2H). IR: ν 2251, 3105 cm^{-1}.

2-(1-(3'-Chlorophenyl)-5-(1*H*-pyrrol-1-yl)-1*H*-pyrazol-4-yl)acetonitrile (46). Was prepared as **50** from **33**. Yield 58% as an oil. ^{1}H NMR (DMSO-d_6): δ ($CDCl_3$): δ 7.82 (s, 1H), 7.24 (m, 2H), 7.17 (t, *J* = 1.9 Hz, 1H), 6.87 (d, *J* = 7.9 Hz, 1H), 6.66(m, 2H), 6.41 (m, 2H), 3.52 ppm (s, 2H). IR: ν 2252, 3105, 3313, 3399 cm^{-1}.

2-[1-(4'-Chlorophenyl)-5-(1*H*-pyrrol-1-yl)-1*H*-pyrazol-4-yl]acetonitrile (47). Was prepared as **50** from **34**. Yield 87% as an oil. ^{1}H NMR (DMSO-d_6): δ 7.91 (s, 1H), 7.46 (d, *J* = 8.8 Hz, 2H), 7.09 (d, *J* = 8.8 Hz, 2H), 6.91 (t, *J* = 2.0 Hz, 2H), 6.31 (t, *J* = 2.0 Hz, 2H), 3.79 ppm. (s, 2H). IR: ν 2252, 3106 cm^{-1}.

2-(1-(2'-Methylphenyl)-5-(1*H*-pyrrol-1-yl)-1*H*-pyrazol-4-yl)acetonitrile (48). Was prepared as **50** from **35**. Yield 35%, mp 58-63 °C (from toluene). ^{1}H (DMSO-d_6): δ 7.86 (s, 1H), 7.32 (m, 4H), 6.77 (m, 2H), 6.15 (m, 2H), 3.82 (s, 2H), 1.95 ppm (s, 3H). IR: ν 2249, 3010, 3117 cm^{-1}.

2-(1-(3'-Methylphenyl)-5-(1*H*-pyrrol-1-yl)-1*H*-pyrazol-4-yl)acetonitrile (49). Was prepared as **50** from **36**. Yield 85%, mp 73-77 °C (from aqueous ethanol). ^{1}H NMR (DMSO-d_6): δ 7.87 (s, 1H), 7.24 (t, *J* = 7.8 Hz, 1H), 7.15 (d, *J* = 7.6 Hz, 1H), 6.94 (s, 1H), 6.88 (m, 2H), 6.83 (d, *J* = 7.8 Hz, 1H), 6.30 (m, 2H), 3.78 (s, 2H), 2.25 ppm (s, 3H). IR: ν 2245 cm^{-1}.

2-[1-(2'-Methoxyphenyl)-5-(1*H*-pyrrol-1-yl)-1*H*-pyrazol-4-yl]acetonitrile (51). Was prepared as **50** from **38**. Yield 81% as an oil. ^{1}H NMR ($CDCl_3$): δ 7.81 (s, 1H), 7.37 (m, 1H), 7.31 (dd, *J* = 1.6 and

7.8 Hz, 1H), 6.99 (t, *J* = 7.6 Hz, 1H), 6.89 (d, *J* = 8.4 Hz, 1H), 6.59 (m, 2H), 6.20 (m, 2H), 3.63 (s, 3H), 3.54 ppm (s, 2H). IR: ν 1601, 2250, 2929, 3105 cm^{-1}

2-[3-Methyl-1-phenyl-5-(1*H*-pyrrol-1-yl)-1*H*-pyrazol-4-yl]acetonitrile (52). Was prepared as **50** from **39**. Yield 58%, mp 100-103 °C (from aqueous ethanol). ^{1}H NMR (DMSO-d_6): δ 7.40-7.25 (m, 3H), 7.05 (m, 2H), 6.87 (dd, *J* = 3.9 and 1.8 Hz, 2H), 6.30 (dd, *J* = 3.9 and 1.8 Hz, 2H), 3.70 (s, 2H), 2.34 ppm (s, 3H). IR: ν 2248 cm^{-1}.

2-[3-Methyl-1-(2'-methylphenyl)-5-(1*H*-pyrrol-1-yl)-1*H*-pyrazol-4-yl]acetonitrile (53). Was prepared as **50** from **40**. It was used as a crude compound.

2-[1-(2'-Chlorophenyl)-3-methyl-5-(1*H*-pyrrol-1-yl)-1*H*-pyrazol-4-yl]acetonitrile (54). Was prepared as **50** from **41**. Yield 89% as an oil. ^{1}H NMR (DMSO-d_6): δ 7.56 (m, 2H), 7.47 (m, 1H), 7.41 (m, 1H), 6.75 (m, 2H), 6.14 (m, 2H), 3.73 (s, 2H), 2.31 ppm (s, 3H). IR: ν 2252, 3104 cm^{-1}.

2-[1-(2',4'-Dichlorophenyl)-3-methyl-5-(1*H*-pyrrol-1-yl)-1*H*-pyrazol-4-yl]acetonitrile (55). Was prepared as **50** from **42**. Yield 93%, mp 105-106 °C (from toluene). ^{1}H NMR (DMSO-d_6): δ 7.77 (d, *J* = 2.2 Hz, 1H), 7.63 (d, *J* = 8.5 Hz, 1H), 7.51 (dd, *J* = 2.3 and 8.5 Hz, 1H), 6.77 (m, 2H), 6.17 (m, 2H), 3.74 (s, 2H), 2.31ppm (s, 3H). IR: ν 2247, 3092 cm^{-1}.

2-[1-(4'-Chloro-2'-methylphenyl)-3-methyl-5-(1*H*-pyrrol-1-yl)-1*H*-pyrazol-4-yl]acetonitrile (56). Was prepared as **50** from **43**. Yield 68% as an oil. ^{1}H NMR (DMSO-d_6): δ 7.40 (s, 1H), 7.26 (s, 2H), 6.78 (m, 2H), 6.16 (m, 2H), 3.72 (s, 2H), 2.31 (s, 3H), 1.95 ppm (s, 3H). IR: ν 2250 cm^{-1}.

General procedure for the synthesis of derivatives 57-67. Example. Ethyl 3-cyano-2-hydroxy-3-[5-(1*H*-pyrrol-1-yl)-1-(4'-methylphenyl)-1*H*-pyrazol-4-yl]acrylate (63). Sodium ethoxide was freshly prepared from sodium metal (0.13 g, 0.0056 ga) in absolute ethanol (3.74 mL). Diethyl oxalate (1.07 mL, 0.99 mL, 0.0078 mol) and **50** (1.47 g, 0.0056 mol) were added in sequence. The reaction was stirred at room temperature for 5 h. The mixture was quenched with water and brought to pH 2 with 1 N HCl. After extraction with ethyl acetate, the combined organic solutions were washed with brine and

dried. Removal of the solvent afforded **63** (1.6 g, yield 81%), mp 157-162 °C (fom aqueous ethanol). ^{1}H NMR (DMSO-d_6): δ 8.08 (s, 1H), 7.16 (d, J = 8.4 Hz, 2H), 6.98 (d, J = 8.4 Hz, 2H), 6.79 (m, 2H), 6.20 (m, 2H), 4.28 (q, J = 7.1 Hz, 2H), 2.29 (s, 3H), 1.28 ppm (t, J = 7.1 Hz, 3H). IR: ν 2222, 3236, 3450 cm^{-1}.

Ethyl 3-cyano-2-hydroxy-3-[5-(1*H*-pyrrol-1-yl)-1-(phenyl)-1*H*-pyrazol-4-yl]acrylate (57). Was prepared as **63** from **44**.[20]

Ethyl 3-[1-(2'-chlorophenyl)-5-(1*H*-pyrrol-1-yl)-1*H*-pyrazol-4-yl]-3-cyano-2-hydroxyacrylate (58). Was prepared as **63** from **45**. Yield 78% as an oil. ^{1}H NMR (DMSO-d_6): δ 8.11 (s, 1H), 7.60 (m, 2H), 7.50 (m, 1H), 7.42 (m, 1H), 6.72 (m, 2H), 6.07 (m, 2H), 4.31 (m, 2H), 1.29 ppm (t, J = 7.1 Hz, 3H). IR: ν 1720, 2222 cm^{-1}.

Ethyl 3-[1-(3'-chlorophenyl)-5-(1*H*-pyrrol-1-yl)-1*H*-pyrazol-4-yl]-3-cyano-2-hydroxyacrylate (59). Was prepared as **63** from **46**. Yield 79% as an oil. ^{1}H NMR (DMSO-d_6): δ 8.19 (s, 1H), 7.23 (t, J = 8.0 Hz, 2H), 7.17 (s, 1H), 6.88 (d, J = 8.4 Hz, 1H), 6.70 (m, 2H), 6.40 (m, 2H), 4.49 (q, J = 7.1 Hz, 2H), 1.44 ppm (t, J = 7.1 Hz, 3H). IR: ν 1718, 2224 cm^{-1}.

Ethyl 3-[1-(4'-chlorophenyl)-5-(1*H*-pyrrol-1-yl)-1*H*-pyrazol-4-yl]-3-cyano-2-hydroxyacrylate (60). Was prepared as **63** from **47**. Yield 62%, mp 59-62 °C (from thyl acetate/*n*-hexane). ^{1}H NMR (DMSO-d_6): δ 8.27 (s, 1H), 7.37 (d, J = 8.6 Hz, 2H), 6.96 (d, J = 8.5 Hz, 2H), 6.77 (s, 2H), 6.19 (s, 2H), 4.15 (dd, J = 7.0 and 14.0 Hz, 2H), 1.22 ppm (t, J = 7.2 Hz, 3H). IR: ν 2261, 3361 cm^{-1}.

Ethyl 3-cyano-2-hydroxy-3-[5-(1*H*-pyrrol-1-yl)-1-(2'-methylphenyl)-1*H*-pyrazol-4-yl]acrylate (61). Was prepared as **63** from **48**. Yield 76%, mp 137-142 °C (from toluene). ^{1}H NMR (DMSO-d_6): δ 8.07 (s, 1H), 7.27 (m, 4H), 6.72 (s, 2H), 6.06 (s, 2H), 4.31 (q, J = 7.0 Hz, 2H), 1.99 (s, 3H), 1.29 ppm (t, J = 7.1 Hz, 3H). IR: ν 1713, 2221, 3107 cm^{-1}.

Ethyl 3-cyano-2-hydroxy-3-[5-(1*H*-pyrrol-1-yl)-1-(3'-methylphenyl)-1*H*-pyrazol-4-yl]acrylate (62). Was prepared as **63** from **49**. Yield 70% as an oil. ^{1}H NMR (DMSO-d_6): δ 8.09 (s, 1H), 7.23 (t, J

= 7.8 Hz, 1H), 7.15 (d, *J* = 7.4 Hz, 1H), 6.93 (s, 1H), 6.85 (d, *J* = 8.3 Hz, 1H), 6.81 (m, 2H), 6.22 (m, 2H), 4.31 (q, *J* = 7.1 Hz, 2H), 2.25 (s, 3H), 1.29 (t, *J* = 7.1 Hz, 3H). IR: ν 1736, 2229, 3153 cm^{-1}.

Ethyl 3-cyano-2-hydroxy-3-[1-(2'-methoxyphenyl)-5-(1H-pyrrol-1-yl)-1H-pyrazol-4-yl]acrylate (64). Was prepared as **63** from **51**. Yield 78% as an oil. ^{1}H NMR ($CDCl_3$): δ 8.14 (s, 1H), 7.41 (m, 1H), 7.24 (m, 1H), 6.98 (d, *J* = 7.4 Hz, 1H), 6.90 (d, *J* = 8.3 Hz, 1H), 6.61 (m, 2H), 6.17 (dd, *J* = 5.9 and 8.0 Hz, 2H), 4.47 (q, *J* = 7.2 Hz, 2H), 3.66 (s, 3H), 1.43 ppm (t, *J* = 7.2 Hz, 3H). IR: ν 1717, 2200, 2963 cm^{-1}.

Ethyl 3-cyano-2-hydroxy-3-[3-methyl-1-phenyl-5-(1*H*-pyrrol-1-yl)-1*H*-pyrazol-4-yl]acrylate (65). Was prepared as **63** from **52**. Yield 36%, mp 57-60 °C (from toluene). ^{1}H NMR (DMSO-d_6): δ 7.33 (m, 5H), 6.75 (m, 2H), 6.22 (m, 2H), 4.30 (q, *J* = 7.1 Hz, 2H), 2.22 (s, 3H), 1.30 ppm (m, 3H). IR: ν 1719, 2217cm^{-1}.

Ethyl 3-cyano-2-hydroxy-3-[3-methyl-5-(1*H*-pyrrol-1-yl)-1-(2'-methylphenyl)-1*H*-pyrazol-4-yl]acrylate (66). Was prepared as **63** from **53.** Yield 57% as an oil. ^{1}H NMR (DMSO-d_6): δ 7.29 (m, 4H), 6.63 (m, 2H), 6.09 (m, 2H), 4.27 (q, *J* = 7.1 Hz, 2H), 2.22 (s, 3H), 1.96 (s, 3H), 1,28 ppm (t, *J* = 7,12 Hz, 3H). IR: ν 1740, 2214 cm^{-1}.

Ethyl 3-cyano-2-hydroxy-3-[3-methyl-5-(1*H*-pyrrol-1-yl)-1-(2'-chlorophenyl)-1*H*-pyrazol-4-yl]acrylate (67). Was prepared as **64** from **54**. t was used as a crude compound.

Ethyl 2-[1-[4-(cyanomethyl)-1-(2',4'-dichlorophenyl)-3-methyl-1*H*-pyrazol-5-yl]-1*H*-pyrrol-2-yl]-2-oxoacetate (68). A mixture of **55** (0.45 g, 0.00137 mol), ethyl 2-chloro-2-oxoacetate (1.12 g, 0.90 mL, 0.0082 mol) in dry toluene (7 mL) was heated at reflux for 6 h. After cooling, water was added and the mixture was extracted with ethyl acetate. The combined organic layers were washed with brine and dried. After evaporation of the solvent, the residue was purified by silica gel column chromatography using ethyl acetate:*n*-hexane 1:1 as eluent, to give **68** (0.58 g, yield 98%) as an oil. ^{1}H NMR (DMSO-d_6): δ 7.75 (s, 1H), 7.52 (s, 1H), 7.48 (d, *J* = 9.0 Hz, 1H), 7.33 (s, 1H), 7.28 (s, 1H), 6.48 (s, 1H), 4.26

(q, *J* = 7.1 Hz, 2H), 3.71 (d, *J* = 3.9 Hz, 2H), 2.32 (s, 3H), 1.25 ppm (t, *J* = 7.1 Hz, 3H). IR: ν 1652, 1732, 2255, 3110 cm^{-1}.

Ethyl 2-[1-[1-(4'-chloro-2'-methylphenyl)-4-(cyanomethyl)-3-methyl-1*H*-pyrazol-5-yl]-1*H*-pyrrol-2-yl]-2-oxoacetate (69). Was prepared as **68** from **56**. Yield 99% as an oil. ^{1}H NMR (DMSO-d_6): δ 7.65 (d, *J* = 1.6 Hz, 1H), 7.40 (d, *J* = 1.9 Hz, 1H), 7.32 (dd, *J* = 4.1 and 1.5 Hz, 1H), 7.20 (dd, *J* = 8.4 and 2.4 Hz, 1H), 7.02 (d, *J* = 8.5 Hz, 1H), 6.49 (dd, *J* = 4.1 and 2.7 Hz, 1H), 4.28 (q, *J* = 7.1 Hz, 2H), 3.68 (d, *J* = 9.5 Hz, 2H), 2.33 (s, 3H), 2.07 (s, 3H), 1.27 ppm (d, *J* = 7.5 Hz, 3H). IR: ν 1651, 1732, 2253, 3115 cm^{-1}.

Ethyl 1-(4'-chloro-2'-methylphenyl)-4-cyano-3-methyl-1*H*-pyrazolo[3,4-*e*]indolizine-5-carboxylate (71). A mixture of **69** (1.36 g, 0.0035 mol) and potassium carbonate (1.19 g, 0.0079 mol) in anhydrous DMF (44 mL) was heated at 100 °C for 4 h. After cooling, water and 1 N HCl were added while stirring. The mixture was extracted with ethyl acetate, washed brine and dried. Removal of the solvent gave a residue that was purified by silica gel column using ethyl acetate:*n*-hexane (1:2) as eluent to afford **71** (0.45 g, yield 32%), mp 115-118 °C (from aqueous ethanol). ^{1}H NMR ($CDCl_3$): δ 7.69 (s, 1H), 7.63 (d, *J* = 8.4 Hz, 1H), 7.56 (d, *J* = 8.4 Hz, 1H), 7.25 (m, 1H), 6.93 (m, 1H), 6.71 (m, 1H), 4.49 (q, *J* = 7.0 Hz, 2H), 2.66 (s, 3H), 1.97 (s, 3H), 1.41 ppm (t, *J* = 7.1 Hz, 3H). IR: ν 1765, 1830, 2220 cm^{-1}.

Ethyl 4-cyano-1-(2',4'-dichlorophenyl)-3-methyl-1H-pyrazolo[3,4-e]indolizine-5-carboxylate (70). Was prepared as **71** from **68**. Yield 53%, mp 127-130° (from aqueous ethanol)**.** ^{1}H NMR (DMSO-d_6): 8.07 (s, 1H), 7.93 (d, *J* = 8.4 Hz, 1H), 7.78 (d, *J* = 8.6 Hz, 1H), 7.28 (m, 1H), 7.97 (m, 1H), 6.85 (s, 1H), 4.49 (q, *J* = 7.0 Hz, 2H), 2.66 (s, 3H), 1.41 ppm (t, *J* = 7.1 Hz, 3H). IR: ν 1710, 1764, 2219 cm^{-1}.

X-ray Structure Selection. Numerous X-ray structures of GSK-3β have been released in the Protein Data Bank (PDB); some of them are co-crystallized with maleimide- or maleimide like-

containing inhibitors (PDB codes: 1Q3D, 1Q41, 1UV5, 1Q4L, 2JLD and 2OW3). A superposition of the mentioned X-ray structures on the alpha carbon atoms, using the 1Q41 as reference (as it possess the highest resolution), showed that the protein folding is largely superimposable, with the exception of the nucleotide-binding loop which adopted different conformations upon ligand binding changing the available room in the catalytic binding site. Compound **5** was docked in three different GSK-3β structures, each one representative for a nucleotide-binding loop conformation: 1UV5[36] (closed conformation), 1Q41[37] ("semiclosed" conformation) and 1Q3D[37] (open conformation).

Molecular Docking. Molecular docking was carried out using the Glide 5.5 program.[38] Maestro 9.0.211[39] was employed as the graphical user interface and Figure 1 and Figure 2 were rendered by the Chimera software package.[40] The 3D structure of **5** was first generated with the Maestro Build Panel and then, a geometry optimized ligand was prepared using Lig-Prep 2.3 as implemented in Maestro. As for the target proteins, hydrogens and other missing atoms were added, and the proteins were energy-minimized using the OPLS-AA 2005 force field within the Protein Preparation Wizard module. Docking calculations of **5** into the GSK-3β active site of the selected X-ray structures (PDB code: 1Q3D, 1UV5 and 1Q41) suggested the same binding pose, thus, in the main text just the pose found in 1Q3D is described.

MC/FEP Calculations. As for the computationally-driven optimization step, relative free energies of binding were predicted by conjugate-gradient energy minimizations and Monte Carlo/FEP (MC/FEP) calculations, executed by means of the MCPRO program[41] following well-established protocols.[25,42] Starting from the docking pose of **5** into GSK-3β, coordinates of analogues of **5** in complex with the enzyme, were generated from the 1Q3D crystal structure using the molecule growing program BOMB. To reduce the computational cost, these complexes were truncated at 15 Å from the ligand and included 138 amino acid residues closest to the catalytic binding site; steric clashes were relieved by short conjugate-gradient minimizations (50 steps). Coordinates for the free ligands were

obtained by extraction from the complexes. The unbound ligands and complexes were hydrated by a sphere of TIP4P water molecules of 25 Å radius containing ca. 2000 and 1250 water molecules for the unbound and bound MC simulations, respectively. The FEP calculations utilized 11 windows of simple overlap sampling,[43] each one covering 10-15 million (M) configurations of equilibration and 10-30 M configurations of averaging at 25 °C. The ligand and side chains with any atom within ca. 10 Å of the ligand were fully flexible, while the protein backbone was kept fixed during the MC runs. The energetics were evaluated with the OPLS-AA force field for the protein,[44] OPLS/CM1A for the ligands,[45] and TIP4P for water.[46]

VOLSURF+ BBB penetration prediction. The overall procedure contained the following four major steps: (i) building of the 3D structure of the compounds; (ii) multivariate characterization based on the interaction energy with the chemical probes; molecular mechanics force fields or semiempirical methods as well as ab initio methods were used by means of GRID program; (iii) molecular descriptors were calculated using the VolSurf+ program; (iv) chemometric tools (PCA, discriminant PLS) were used to correlate the data and with the Crivori BBB permeation model. Step (ii) was automatically performed by the VolSurf+ program and the molecules were considered in their neutral form. Only a small fraction (~20%) was in the deprotonated form, as predicted by MarvinSketch (ChemAxon).

GSK-3β in Vitro Assay. Purified GSK-3β (0.5 μg) was incubated in a reaction mixture of 50 mM Tris pH 7.3, 10 mM MgAc2, 0.01% β-mercaptoethanol, ^{32}P[γ-ATP](100 μM, 0.5 μci/assay), and 100 μM of peptide substrate, pIRS-1 (RREGGMSRPAS(p)VDG (1). New molecules were added at various concentrations (0.1-100 μM), and the reaction mixture was incubated for 15 min at 30 °C. The reactions were stopped, spotted on p81 paper (Whatman), washed with 10 mM phosphoric acid, and counted for radioactivity.[47] GSK-3β activity was calculated as the percentage of GSK-3β activity in the

absence of inhibitor that was designated to 100%. IC_{50} values were calculated as the concentration in which 50% inhibition is achieved.

CDK2 Assay. The experiments were carried out in duplicate with 8 concentrations of the inhibitor using human recombinant CDK2. Purified CDK2 was incubated in the presence of ATP and Ulight-CFFKNIVTPRTPPPSQGK-amide (50 nM). New inhibitor was added, and the reaction mixture was incubated for 30 min at room temperature. The kinase activity was measured by detecting the phospho-Ulight-CFFKNIVTPRTPPPSQGK-amide component (LANCE method). Staurosporin (IC_{50} = 5.4 nM) was used as reference compound (see Table 1S of the Supporting Information).

Human Protein Kinase Assays. The experiments were carried out using human recombinant kinases. The experimental conditions for each measurement of kinase inhibition are depicted in Table 2S and Table 3S of the Supporting Information.

Tau Fibril Preparation. Fibrils comprised of 5'-mycK18PL tau were prepared as previously described.[48,49]

Inducible Tau Cell line. A stable HEK/QBI293 clone stably expressing tTA under the control of a doxycycline-inducible promoter was transfected with pLVXtight carrying 2N4R tau (T40) containing the P301L mutation to obtain a clonal cell line that stably expresses doxycycline-inducible tau (Dox-T40PL). Briefly, QBI293 cells (ATCC) were transfected with lentivirus containing the rtTA plasmid (Clontech) and stable clones were selected. A resulting stably-transfected rtTA clone was subsequently transfected with the pLVXtight puro plasmid (Clontech) into which T40P301L had been cloned. These cells were subjected to two rounds of cloning to obtain the stable Dox-T40PL clone. The Dox-T40PL cells were grown in DMEM supplemented with 10% tetracycline-free FBS, 1% L-glutamine, 1%

pen/strep antibiotic mix, 400 μg/mL G418 (selection for rtTA construct), and 1.25 μg/mL puromycin (selection for pLVXtight construct). Tau expression in the Dox-T40PL cells was induced by the addition of 1 μg/mL doxycycline to the growth medium.

Fibril Transduction and Compound Treatment. Dox-T40PL cells were seeded at 100,000/mL in 2 mL per well in a 6-well plate and tau expression was induced for 48 h prior to transduction with 5'mycK18PL fibrils. A 40 μM preparation of 5'-mycK18PL fibrils was diluted to 10 μM with 100 mM sodium acetate, pH 7.0, followed by sonication with 60 pulsed with a QSonica XL-2000 Model CML-4 microtip sonicator at setting 2. An 80 μL aliquot of the sonicated fibrils was added to one tube of lyophilized Genlantis BioPorter Quickease (for 96 well plates) and gently triturated five times, followed by gentle vortexing for 5 seconds. The fibril-BioPorter mix was then incubated at room temperature for 10 min. The Dox-T40PL cells were washed once with 0.5 mL of transduction medium (Opti-MEM reduced serum medium (Invitrogen) with 1 μg/mL doxycycline added), followed by addition of 0.5 mL of transduction medium. An 80 μL aliquot of the tau fibril-BioPorter mixture was added to 420 μL of transduction medium, and this mixture was added to the cells followed by a 3 h incubation at 37 °C. The cells were subsequently dissociated with trypsin, spun and resuspended in growth medium containing doxycycline. After performing a cell count, 1 mL of the cell suspension containing 73,000 cells/mL was plated per well in a 12-well plate. The replated Dox-T40PL cells were treated with 1 μM test compounds resuspended in DMSO, or DMSO alone, followed by an additional 48 h of incubation before lysis.

Cell Lysis and Immunblotting. Cells were rinsed with ice-cold phosphate-buffered saline, followed by addition of 80 μL of cell lysis buffer (50 mM Tris, pH 7.6,2% SDS, 150 mM NaCl, 0.1 mM PMSF with 0.1% protease inhibitor cocktail (100 μg/mL each of pepstatin A, leupeptin, TPCK, TLCK, and soybean trypsin inhibitor and 100 mM EDTA) and phosphatase inhibitor). Cells were

scraped into a tube and sonicated to prepare a cellular homogenate, and protein content was determined using a BCA assay. Equal amounts of cellular homogenates (25 μg of protein) were loaded per lane on a 10% acrylamide SDS-PAGE gel. Following electrophoresis, samples were electro-blotted onto nitrocellulose, and the nitrocellulose was cut at the site of the 50 kD molecular weight marker. The upper half of the nitrocellulose (containing the tau) was stained with the antibodies 17025 (a rabbit polyclonal antibody raised to 2N4R tau) and AT180 (a mouse monoclonal antibody which recognizes pS231/pT235 tau (Thermo Scientific) residues). The lower half of the nitrocellulose (containing the GAPDH) was stained with an anti-GAPDH monoclonal antibody (Advanced Immunochemical). The primary antibodies were detected with anti-rabbit or anti-mouse IgG IRDye secondary antibodies (LiCor), followed by imaging on a LiCor chemiluminescence reader. Bands were quantified using Image Quant 5.0 software. All bands were normalized to GAPDH.

Aqueous solubility. The solubility in aqueous pH 7.4 buffer of compounds **18** was measured in a shake-flask assay after incubation for 24 h at room temperature using HPLC-UV/VIS as a detection method (see Table 4S of the Supporting Information).

ASSOCIATED CONTENT

Supporting Information Available. Additional chemical and biological material is available free of charge via the internet at http//pubs.acs.org.

ACKNOWLEDGMENT

Authors thank dr. Ernest Hamel, National Cancer Institute, National Institutes of Health, Frederick, Maryland 21702, United States, for the evaluation of compound **18** in parental OVCAR-8 and P-gp overexpressing NCI/ADR-RES cell lines. This research was supported by PRIN 2010-2011 (grant No. 2010W7YRLZ), Progetti di Ricerca di Università, Sapienza Università di Roma (grant year 2012), and Bando Futuro in Ricerca 2010 (grant No. RBFR10ZJQT). This research was also supported by Israel Science Foundation grant No. 341/10. A. C. was partially supported by FIRB grant No. RBIN06E9Z8. We thank prof. Gabriele Cruciani for helpful discussion on the VolSurf procedure and for providing the VOLSURF+ license.

AUTHOR INFORMATION

*__Corresponding Authors.__ G.L.R.: Phone +39 06 4991 3404, Fax +39 06 4969 3268, E-mail giuseppe.laregina@uniroma1.it; L.M.: Phone +39 081 678619, Fax +39 081 676569, E-mail luciana.marinelli@unina.it.

ABBREVIATIONS

AD, Alzheimer's disease; GSK-3, glycogen synthase kinase-3; FEP, free energy perturbation; MC, monte carlo.

REFERENCES

(1) Alzheimer's Association. 2009 Alzheimer's disease facts and figures. *Alzheimers Dement.* **2012**, *8*, 131-168.

(2) (a) Arriagada, P. V.; Growdon, J. H.; Hedley-Whyte, E. T.; Hyman, B. T. Neurofibrillary tangles but not senile plaques parallel duration and severity of Alzheimer's disease. *Neurology* **1992**, *42*, 631-639. (b) Arriagada, P. V.; Marzloff, K.; Hyman, B. T. Distribution of Alzheimer-type pathologic changes in nondemented elderly individuals matches the pattern in Alzheimer's disease. *Neurology* **1992**, *42*, 1681-1688.

(3) Hardy, J. Alzheimer's disease: the amyloid cascade hypothesis: an update and reappraisal. *J. Alzheimers Dis.* **2006**, *9*, 151-153.

(4) Zaghi, J.; Goldenson, B.; Inayathullah, M.; Lossinski, S.; Masoumi, A.; Avagyan, H.; Mahanian, M.; Bernas, M.; Weinand, M.; Rosemnthal, M. J.; Espinosa-Jeffrey, A.; Vellis, J.; Teplov, D. B.; Fiala, M. Alzheimer disease macrophages shuttle amyloid-beta from neurons to vessels, contributing to amyloid angiopathy. *Acta Neuropthol*. **2009**, *117*, 111-124.

(5) Gilstad, J. R.; Finucane, T. E. Results, rhetoric, and randomized trials: the case of donepezil. *J. Am. Geriatr. Soc.* **2008**, *56*, 1556-1562.

(6) Jope, R. S.; Johnson, G. V. The glamour and gloom of glycogen synthase kinase-3. *Trends Biochem. Sci.* **2004**, *29*, 95-102.

(7) Ferreira, A.; Lu, Q.; Orecchio, L.; Kosik, K. S. Selective phosphorylation of adult tau isoforms in mature hippocampal neurons exposed to fibrillar A beta. *Mol. Cell. Neurosci.* **1997**, *9*, 220-234.

(8) Embi, N.; Rylatt, D. B.; Cohen, P. Glycogen synthase kinase-3 from rabbit skeletal muscle. Separation from cyclic-AMP-dependent protein kinase and phosphorylase kinase. *Eur. J. Biochem.* **1980**, *107*, 519-527.

(9) Forde, J. E.; Dale, T. C. Glycogen synthase kinase 3: a key regulator of cellular fate. *Cell Mol. Life Sci.* **2007**, *64*, 1930-1944.

(10) Martinez, A.; Castro, A.; Medina, M. *Glycogen synthase kinase 3 and its inhibitors: Drug discovery and developments*; John Wiley & Sons: New York, 2006; pp. 105-124.

(11) (a) Ilyas, M. Wnt signalling and the mechanistic basis of tumour development. *J. Pathol.* **2005**, *205*, 130-144; (b) Dale, T. C. Signal transduction by the Wnt family of ligands. *Biochem. J.* **1998**, *329*, 209-223.

(12) King, T. D.; Clodfelder-Miller, B.; Barksdale, A.; Bijur, G. N. Unregulated mitochondrial GSK3beta activity results in NADH: ubiquinone oxidoreductase deficiency. *Neurotox Res.* **2008**, *14*, 367-382.

(13) Yang, W.; Leystra-Lantz, C.; Strong, M. J. Upregulation of GSK3beta expression in frontal and temporal cortex in ALS with cognitive impairment (ALSci). *Brain Res.* **2008**, *1196*, 131-139.

(14) (a) Woodgett, J. R. Molecular cloning and expression of glycogen synthase kinase-3/factor A. *Embo J.* **1990**, *9*, 2431-2438; (b) Woodgett, J. R. cDNA cloning and properties of glycogen synthase kinase-3.. *Methods Enzymol.* **1991**, *200*, 564-577.

(15) Doble, B. W.; Patel, S.; Wood, G. A.; Kockeritz, L. K.; Woodgett, J. R. Functional redundancy of GSK-3alpha and GSK-3beta in Wnt/beta-catenin signaling shown by using an allelic series of embryonic stem cell lines. *Dev. Cell.* **2007**, *12*, 957-971.

(16) Mazanetz, M. P.; Fischer, P. M. Untangling tau hyperphosphorylation in drug design for neurodegenerative diseases. *Nature Rev. Drug Discov.* **2007**, *6*, 464-479.

(17) (a) Bhat, R. V.; Budd Haeberlein, S. L.; Avila, J. Glycogen synthase kinase 3: a drug target for CNS therapies. *J. Neurochem.* **2004**, *89*, 1313-1317; (b) Berg, S.; Bergh, M.; Hellberg,S.; Högdin, K.; Lo-Alfredsson, Y.; Söderman, P.; von Berg, S.; Weigelt, T.; Ormö, M.; Xue, Y.;

Tucker, J.; Jan Neelissen, J.; Jerning, E.; Nilsson, Y.; Bhat, R. Discovery of novel potent and highly selective glycogen synthase kinase-3β (GSK3β) inhibitors for Alzheimer's disease: design, synthesis, and characterization of pyrazines. *J. Med. Chem.* **2012**, *55*, 9107-9119.

(18) Eldar-Finkelman, H.; Martinez, A. GSK-3 inhibitors: Preclinical and clinical focus at the CNS. *Front. Mol. Neurosci.* **2011**, *4*, 32.

(19) (a) Meijer, L.; Flajolet, M.; Greengrad, P. Pharmacological inhibitors of glycogen synthase kinase 3. *Trends Pharmacol. Sci.* **2004**, *25*, 471-480; (b) Kypta, R. M. Review: GSK3 inhibitors and their potential in the treatment of Alzheimer's disease. *Expert Opin. Ther. Pat.* **2005**, *15*, 1315−1331; (c) Martinez, A. Preclinical efficacy on GSK-3 inhibitors: towards a future generation of powerful drugs. *Med. Res. Rev*. **2008**, *28*, 773-796; (d) Lo Monte, F.; Kramer, T.; Gu, J.; Anumala, UR.; Marinelli, L.; La Pietra, V.; Novellino, E.; Franco, B.; Demedts, D.; Van Leuven, F.; Fuertes, A.; Dominguez, J.M.; Plotkin, B.; Eldar-Finkelman, H.; Schmidt, B. Identification of glycogen synthase kinase-3 inhibitors with a selective sting for glycogen synthase kinase-3α. *J. Med. Chem.* **2012**, *55*, 4407-4424.

(20) Artico, M.; Massa, S.; Stefancich, G.; Silvestri, R.; Di Santo, R.; Corelli, F. Synthesis of pyrazolo[3,4-*e*]pyrrolo[3.4-e]indolizine and 1*H*-pyrazolo[3,4-*e*]indolizine derivatives. *J. Heterocyclic Chem.* **1989**, *26*, 503-507.

(21) Polychronopoulos, P.; Magiatis, P.; Skaltsounis, A.-L.; Myrianthopoulos, V.; Mikros, E.; Tarricome, E.; Musacchio, A.; Roe, S. M.; Pearl, L.; Leost, M.; Greengard, P.; Meijer, L. Structural basis for the synthesis of indirubins as potent and selective inhibitors of glycogen synthase kinase-3 and cyclin-dependent kinases.. *J. Med. Chem.* **2004**, *47*, 935-946.

(22) Coghlan, M. P.; Culbert, A. A.; Cross, D. A. E.; Corcoran, S. L.; Yates, J. W.; Pearce, N. J.; Rausch, O. L.; Murphy, G. J.; Carter, P. S.; Cox, L. R.; Mills, D.; Brown, M. J.; Haigh, D; Ward, R. W.; Smith, D. G.; Murray, K. J.; Reith, A. D.; Holder, J. C. Selective small molecule

inhibitors of glycogen synthse kinase-3 modulate glycogen metabolism and gene transcription. *Chem. Biol.* **2000**, *7*, 793-803.

(23) Lum, C.; Kahl, J.; Kessler, L.; Kucharski, J.; Lundström, J.; Miller, S.; Nakanishi, H.; Pei, Y.; Pryor, K.; Roberts, E.; Sebo, L.; Sullivan, R.; Urban, J.; Wang, Z. 2,5-Diaminopyrimidines and 3,5-disubstituted azapurines as inhibitors of glycogen synthase kinase-3 (GSK-3). *Bioorg. Med. Chem. Lett.* **2008**, *18*, 3578-3581.

(24) Leost, M.; Schultz, C.; Link, A.; Wu, Y.-Z.; Biernat, J.; Mandelkow, E.-M.; Bibb, J. A.; Snyder, G. L.; Greengard, P; Zaharevitz, D. W.; Gussio, R.; Senderowicz, A. M.; Sausville, E. A.; Kunick, C.; Meijer, L. Paullones are potent inhibitors of glycogen synthase kinase-3β and cyclin-dependent kinase 5/p25. *Eur. J. Biochem.* **2000**, *267*, 5983-5959.

(25) Jorgensen W. L. Efficient drug lead discovery and optimization. *Acc. Chem. Res.* **2009**, *42*, 724-733.

(26) Clauson-Kaas, N.; Tyle, Z. Preparation of *cis* and *trans* 2,5-dimethoxy-2-(acetamidomethyl)-2,5-dihydrofuran, *cis* and *trans* 2,5-dimethoxy-2-(acetamidomethyl)-tetrahydrofuran and 1-phenyl-2-(acetamidomethyl)-pyrrole. *Acta Chem. Scand.* **1952**, *6*, 667-670.

(27) Zhang, N.; Zhong, R.; Yan, H.; Jiang, Y. Structural features underlying selective inhibition of GSK3β by dibromocantharelline: implications for rational drug design. *Chem. Biol. Drug. Des.* **2011**, *77*, 199−205.

(28) Hong, M.; Zhukareva, V.; Vogelsberg-Ragaglia, V.; Wszolek, Z.; Reed, L.; Miller, B. I.; Geschwind, D. H.; Bird, T. D.; McKeel, D.; Goate, A.; Morris, J. C.; Wilhelmsen, K. C.; Schellenberg, G. D.; Trojanowski, J. Q.; Lee, V. M. Mutation-specific functional impairments in distinct tau isoforms of hereditary FTDP-17. *Science* **1998**, *282*, 1914-1917.

(29) Hutton, M.; Lendon, C. L.; Rizzu, P.; Baker, M.; Froelich, S.; Houlden, H.; Pickering-Brown, S.; Chakraverty, S.; Isaacs, A.; Grover, A.; Hackett, J.; Adamson, J.; Lincoln, S.; Dickson, D.;

Davies, P.; Petersen, R. C.; Stevens, M.; de Graaff, E.; Wauters, E.; van Baren, J.; Hillebrand, M.; Joosse, M.; Kwon, J. M.; Nowotny, P.; Che, L. K.; Norton, J.; Morris, J. C.; Reed, L. A.; Trojanowski, J.; Basun, H.; Lannfelt, L.; Neystat, M.; Fahn, S.; Dark, F.; Tannenberg, T.; Dodd, P. R.; Hayward, N.; Kwok, J. B.; Schofield, P. R.; Andreadis, A.; Snowden, J.; Craufurd, D.; Neary, D.; Owen, F.; Oostra, B. A.; Hardy, J.; Goate, A.; van Swieten, J.; Mann, D.; Lynch, T.; Heutink P. Association of missense and 5'-splice-site mutations in tau with the inherited dementia FTDP-17. *Nature* **1998**, *393*, 702-705.

(30) Guo, J. L.; Lee, V. M. Seeding of normal Tau by pathological Tau conformers drives pathogenesis of Alzheimer-like tangles. *J. Biol. Chem.* **2011**, *286*, 15317-15331.

(31) Cavallini, A.; Brewerton, S.; Bell, A.; Sargent, S.; Glover, S.; Hardy, C.; Moore, R.; Calley, J.; Ramachandran, D.; Poidinger, M.; Karran, E.; Davies, P.; Hutton, M.; Szekeres, P.; Bose, S.; An unbiased approach to identifying tau kinases that phosphorylate tau at sites associated with Alzheimer's disease. *J. Biol. Chem.* **2013**, *288*, 23331-23347.

(32) Pajouhesh, H.; Lenz, G. R. Medicinal chemical properties of successful central nervous system drugs. *NeuroRx* **2005**, *2*, 541–553.

(33) Wager, T.T.; Chandrasekaran, R.Y.; Hou, X.; Troutman, M. D.; Verhoest, P. R.; Villalobos, A.; Will, Y.; Defining desirable central nervous system drug space through the alignment of molecular properties, in vitro ADME, and safety attributes. *ACS Chem. Neurosci.* **2010**, *1*, 420–434.

(34) Crivori, P.; Cruciani, G.; Carrupt, P. A.; Testa, B.; Predicting blood-brain barrier permeation from three-dimensional molecular structure. *J. Med. Chem.* **2000**, *43*, 2204–2216.

(35) Cross, S.; Cruciani, G.; Molecular fields in drug discovery: getting old or reaching maturity? *Drug Disc. Today* **2010**, *15*, 23–32.

(36) Meijer, L.; Skaltsounis, A. L.; Magiatis, P.; Polychronopoulous, P.; Knockaert, M.; Leost, M.;

Ryan, X. P.; Vonica, C. A.; Brivanlou, A.; Dajani, R.; Crovace, C.; Tarricone, C.; Musacchio, A.; Roe, S. M.; Pearl, L. H.; Greengard, P. GSK-3 selective inhibitors derived from Tyrian purple indirubins. *Chem. Biol.* **2003**, *10*, 1255-1266.

(37) Bertrand, J. A.; Thieffine, S.; Vulpetti, A.; Cristiani, C.; Valsasina, B.; Knapp, S.; Kalisz, H. M.; Flocco, M. Structural characterization of the GSK-3beta active site using selective and non-selective ATP-mimetic inhibitors. *J. Mol. Biol.* **2003**, *333*, 393-407.

(38) Glide, Version 5.5. Schrödinger, LLC, New York, NY, 2009.

(39) Maestro, Version 9.0.211. Schrodinger, L.L.C., New York, NY, 2009.

(40) Pettersen, E. F.; Goddard, T. D.; Huang, C. C.; Couch, G. S.; Greenblatt, D. M.; Meng, E. C.; Ferrin, T. E. UCSF chimera e a visualization system for exploratory research and analysis. *J. Comput. Chem.* **2004**, *25*, 1605-1612.

(41) Jorgensen, W. L.; Tirado-Rives, J. Molecular modeling of organic and biomolecular systems using BOSS and MCPRO. *J. Comput. Chem.* **2005**, *26*, 1689-1700.

(42) (a) Zeevaart, J. G.; Wang, L.; Thakur, V. V.; Leung, C. S.; Tirado-Rives, J.; Bailey, C. M.; Domaoal, R. A.; Anderson, K. S.; Jorgensen, W. L. Optimization of azoles as anti-HIV agents guided by free-energy calculations. *J. Am. Chem. Soc.* **2008**, *130*, 9492–9499; (b) Leung, C. S.; Zeevaart, J. G.; Domaoal, R. A.; Bollini, M.; Thakur, V. V.; Spasov, K.; Anderson, K. S.; Jorgensen, W. L. Eastern extension of azoles as non-nucleoside inhibitors of HIV-1 reverse transcriptase; cyano group alternatives. *Bioorg. Med. Chem. Lett.* **2010**, *20*, 2485–2488.

(43) Jorgensen, W. L.; Thomas, L. T. Perspective on free-energy perturbation calculations for chemical equilibria. *J. Chem. Theory Comput.* **2008**, *4*, 869–876.

(44) Jorgensen, W. L.; Maxwell, D. S.; Tirado-Rives J. Development and testing of the OPLS all-atom force field on conformational energetics and properties of organic liquids. *J. Am. Chem. Soc.* **1996**, *118*, 11225–11236.

(45) Jorgensen, W. L.; Tirado-Rives J. Potential energy functions for atomic-level simulations of water, and organic and biomolecular systems. *Proc. Natl. Acad. Sci. USA* **2005**, *102*, 6665-6670.

(46) Jorgensen, W. L.; Chandrasekhar, J.; Madura, J. D.; Impey, R. W.; Klein, M. L. Comparison of simple potential functions for simulating liquid water. *J. Chem. Phys.* **1983**, *79*, 926–935.

(47) Liberman, Z.; Eldar-Finkelman, H. Serine 332 phosphorylation of insulin receptor substrate-1 by glycogen synthase kinase-3 attenuates insulin signaling. *J. Biol. Chem.* **2005**, *280*, 4422−4428.

(48) Crowe, A.; Ballatore, C.; Hyde, E.; Trojanowski, J. Q.; Lee, V. M. High throughput screening for small molecule inhibitors of heparin-induced tau fibril formation. *Biochem. Biophys. Res. Commun.* **2007**, *358*, 1-6.

(49) Crowe, A.; Huang, W.; Ballatore, C.; Johnson, R. L.; Hogan, A. M.; Huang, R.; Wichterman, J.; McCoy, J.; Huryn, D.; Auld, D. S.; Smith, A. B. 3rd.; Inglese, J.; Trojanowski, J. Q.; Austin, C. P.; Brunden, K. R.; Lee, V. M. Identification of aminothienopyridazine inhibitors of tau assembly by quantitative high-throughput screening. *Biochemistry* **2009**, *48*, 7732-7745.

TOC Graphic